


Resting natural killer cells promote the progress of colon cancer liver metastasis by elevating tumor-derived sSCF

Chenchen Mao, Yanyu Chen, Dong Xing, Teming Zhang, Dianfeng Mei, Zheng Han, Wangkai Xie, Cong Long, Yangxuan Lin, Jiaye Yu, Dan Xiang , Mingdong Lu , Xian Shen , Xiangyang Xue 

Department of General Surgery, The Second Affiliated Hospital and Yuying Children's Hospital of Wenzhou Medical University, Wenzhou, China • Department of Microbiology and Immunology, Institute of Molecular Virology and Immunology, School of Basic Medical Sciences, Wenzhou Medical University, Wenzhou, China • Department of Pediatric Thoracic Surgery, The Second Affiliated Hospital and Yuying Children's Hospital of Wenzhou Medical University, Wenzhou, China • Department of Thoracic Surgery, The First Affiliated Hospital of Wenzhou Medical University, Wenzhou, China • Department of General Surgery, The First Affiliated Hospital of Wenzhou Medical University, Wenzhou, China

 https://en.wikipedia.org/wiki/Open_access

 Copyright information

Abstract

Purpose

The abundance and biological contribution of Natural killer (NK) cells in cancer are controversial. Here, we aim to uncover clinical relevance and cellular roles of NK cells in colon cancer liver metastasis (CCLM)

Methods

We integrated single-cell RNA sequencing, spatial transcriptomics, and bulk RNA-sequencing datasets to investigate NK cells' biological properties and functions in the microenvironment of primary and liver metastatic tumors. Results were validated through an in vitro co-culture experiment based on bioinformatics analysis.

Results

We used single-cell RNA sequencing and spatial transcriptomics to map the immune cellular landscape of colon cancer and well-matched liver metastatic cancer. We discovered that GZMK⁺ resting NK cells increased significantly in tumor tissues and were enriched in the tumor regions of both diseases. After combining bulk RNA and clinical data, we observed that these NK cell subsets contributed to a worse prognosis. Meanwhile, KIR2DL4⁺ activated NK cells exhibited the opposite position and relevance. Pseudotime cell trajectory analysis revealed the evolution of activated to resting NK cells. In vitro experiments further confirmed that tumor-cell-co-cultured NK cells exhibited a resting status, as evidenced by

decreased KIR2DL4 expression. Functional experiments finally revealed that NK cells exhibited tumor-activating characteristics by promoting the dissociation and release of SCF on the tumor cells membrane depending on cell-to-cell interaction, as the supernatant of the co-culture system enhanced tumor progression.

Conclusion

Together, our findings revealed a population of protumorigenic NK cells that may be exploited for novel therapeutic strategies to improve therapeutic outcomes for patients with CCLM.

eLife assessment

This **useful** study draws on published single-cell and spatial transcriptomic data of colon cancer liver metastasis to clarify the pro- and anti-tumorigenic properties of NK cells. The authors discover increased GZMK⁺ resting NK cells in the tumor tissue and reduced abundance of KIR2DL4⁺ activated NK cells. However, the evidence is currently **incomplete**, as the models used to validate the hypothesis and claims are **inadequate** and lack necessary controls.

<https://doi.org/10.7554/eLife.97201.1.sa2>

Introduction

Colon cancer is one of the most common malignancies, with more than 1 million new cases and 500 thousand deaths reported globally in 2020 (Sung et al., 2021 [↗](#)). Approximately 19–26% of patients with colon cancer present with synchronous metastatic diseases at the first diagnosis (Siegel et al., 2020 [↗](#)), among which 14.5–17.5% develop liver metastasis (Siegel, Miller, 2020, Wang et al., 2023 [↗](#)). Although progress in the treatment of metastatic disease, including improved diagnosis and treatment strategies for liver metastases (Chua et al., 2011 [↗](#), Zampino et al., 2016 [↗](#), Ruers et al., 2017 [↗](#)), increased cancer-directed surgery (Wancata et al., 2016 [↗](#)), and the development of targeted therapies (Piawah et al., 2019), has greatly improved the survival of these patients in recent decades, the 2-year relative survival rate for patients diagnosed with distant-stage disease was 36% (Siegel, Miller, 2020), significantly lower than those without metastasis. Thus, colon cancer-derived liver metastasis (CCLM) is a clinical challenge that requires urgent development of novel treatment methods.

The tumor microenvironment (TME) is a dynamic environment that governs tumor behavior and is required for tumor cell survival, growth, proliferation, and metastasis (Yao et al., 2023 [↗](#)). Unlike previous understanding, it has recently been proposed that certain immune cells present in the TME (such as myeloid-derived suppressor cells (Liu et al., 2023 [↗](#)), macrophages (Ngambenjawong et al., 2017 [↗](#)), neutrophils (Li et al., 2019 [↗](#)), and CD8⁺ T cells (Tiberti et al., 2022 [↗](#))) favor tumor progression. Thus, the contradictory findings of the pro- and anti-tumor effects of tumor-infiltrating immune cells require a better understanding of the immune features and profile heterogeneity of CCLM for the future development of immune- modulatory strategies to stratify and target immune cells.

Natural killer (NK) cells, an important component of tumor-infiltrating immune cells, are cytotoxic lymphocytes that play a key role in recognizing and eliminating malignant cells and are therefore considered the early responders against tumors (Maskalenko et al., 2022 [↗](#)). Among various immune cells, tumor-infiltrating NK cells are associated with prognosis in various cancers, such as colorectal cancer (CRC) (Zhong et al., 2022 [↗](#)), lung cancer (Villegas et al., 2002 [↗](#)), and gastric cancer (Ishigami et al., 2000 [↗](#)). Recently, based on their anti-tumor potential, NK cells were exploited for treating malignancies and have proven to be highly promising for the treatment of certain hematologic malignancies (Lamb et al., 2021 [↗](#), Liu et al., 2020 [↗](#)) but have limited efficacy for treating solid tumors (Zhang et al., 2024 [↗](#), Hu et al., 2019 [↗](#), Oh et al., 2019 [↗](#)). Additionally, intratumor NK cells differ phenotypically or functionally from peripheral NK cells in several malignancies (Bruno et al., 2013 [↗](#), Carrega et al., 2008 [↗](#)); a specific subset of tumor-infiltrating NK cells (CD11b[−] and CD27[−]) was associated with tumor progression in lung and hepatocellular cancers (Zhang et al., 2017 [↗](#), Jin et al., 2013 [↗](#)). Notably, the tumor-promoting transformation of NK cells may be educated by cancer cells (Chan et al., 2020 [↗](#), Huergo-Zapico et al., 2018 [↗](#)). However, their function remains elusive. In particular, the presence of specific NK cell subsets within colon cancer and their potential relationship to CCLM progression have not been fully characterized to date.

In this study, we combined previously published single-cell RNA sequencing, spatial transcriptomics (ST), and bulk RNA-sequencing data from public datasets, aiming to comprehensively chart the cellular landscape of TME in primary colon cancer and matched liver metastasis. Results of bioinformatics analysis were further validated through an in vitro co-culture experiment (Fig. 1A [↗](#)).

Results

Integrated scRNA-seq and ST Precisely Quantified Immune Cell Diversity in CCLM

We used a previously published single-cell dataset containing 89 samples from paired samples of colon cancer, adjacent colon, liver metastasis, adjacent liver, lymph nodes along colons, and peripheral blood mononuclear cells from 20 patients to define the heterogeneous immune microenvironment landscapes of CCLM. Subsequently, 178,630 CD45⁺ cells were integrated.

To further define the main cell type, clustering analysis and SingleR were performed, and monocytes, neutrophil cells, native B cells, plasma cells, T cells, and NK cells were identified from the CCLM samples (Fig. 1B–C [↗](#); Fig. S1A and B). Notably, T and NK cells were the major components of all immune cells and distinct across different tissue types, with NK cells significantly decreasing in tumor tissues (both primary colon cancer and liver metastasis cancer) compared to corresponding adjacent normal tissues, whereas T cells were the opposite (Fig. 1D and E [↗](#); Fig. S1C).

To comprehensively analyze the spatial distribution profile of colon primary tumors and CCLM tumors, we collected ST data, which came from eight samples including paired primary colon cancer and liver metastasis. Unsupervised clustering analysis was first performed to cluster similar ST spots, and the annotation of the clusters was further determined according to cell marker genes (Fig. S2A–C). Further, after combining the gene expression features of each sample (Fig. S3) and H&E staining, six morphological regions, including tumor, fibroblast, smooth muscle, B cells, hepatocytes, normal epithelium, and tumor and paratumor areas, were identified. (Fig. 2A–C [↗](#)).

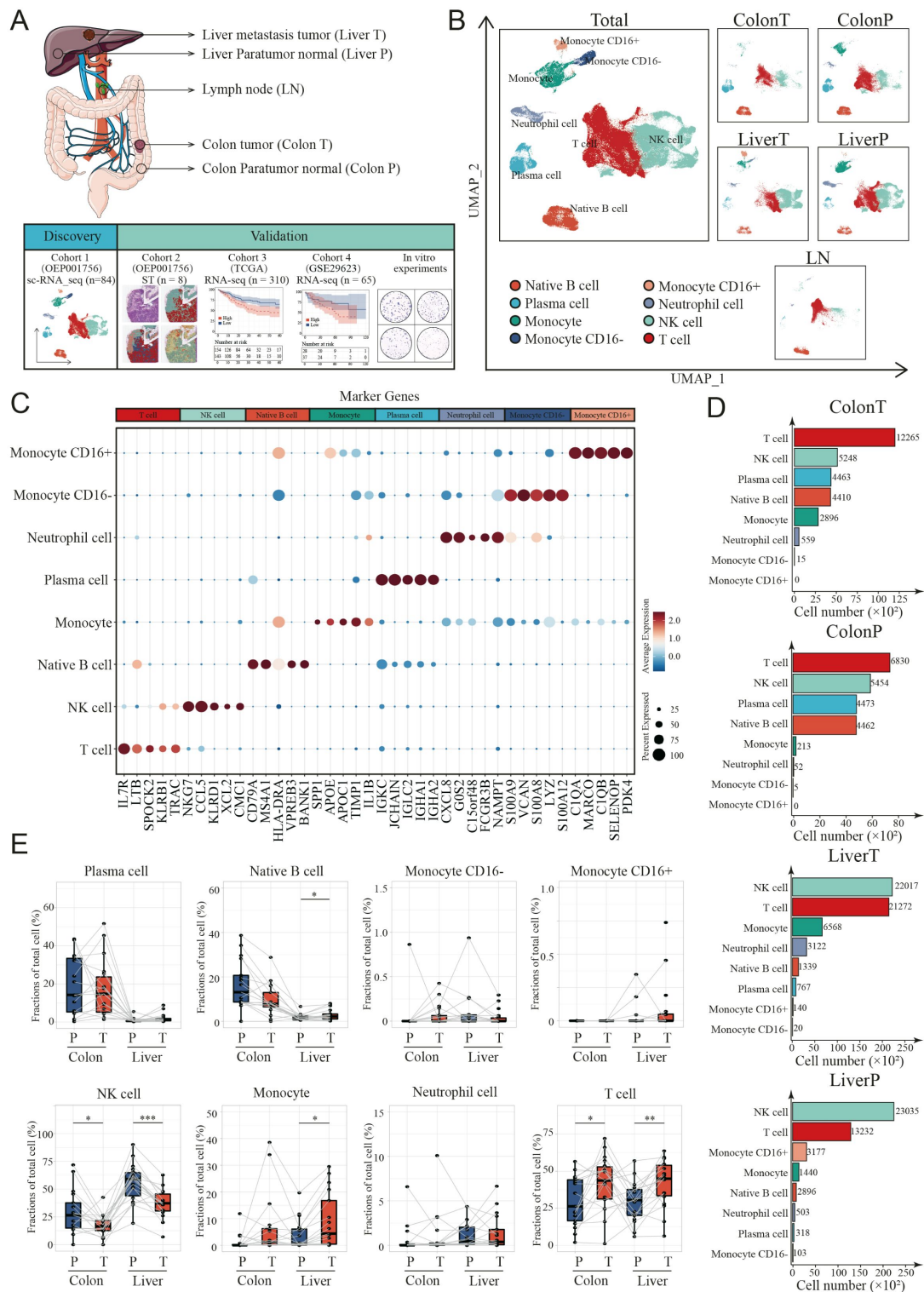


Figure 1.

Landscape of tumor immune microenvironment in CCLM revealed by single-cell transcriptomics. **A.** Schematic overview of the experimental design and analytical workflow. **B.** The UMAP plot of all main immune cell types. **C.** Dot plots showing average expression of known markers in indicated cell clusters. The dot size represents percent of cells expressing the genes in each cluster and the color of dot represents the expression intensity. **D.** The cell numbers of main immune cells across tissues. **E.** Proportions of all main immune cells. P values were determined by the paired nonparameter test.

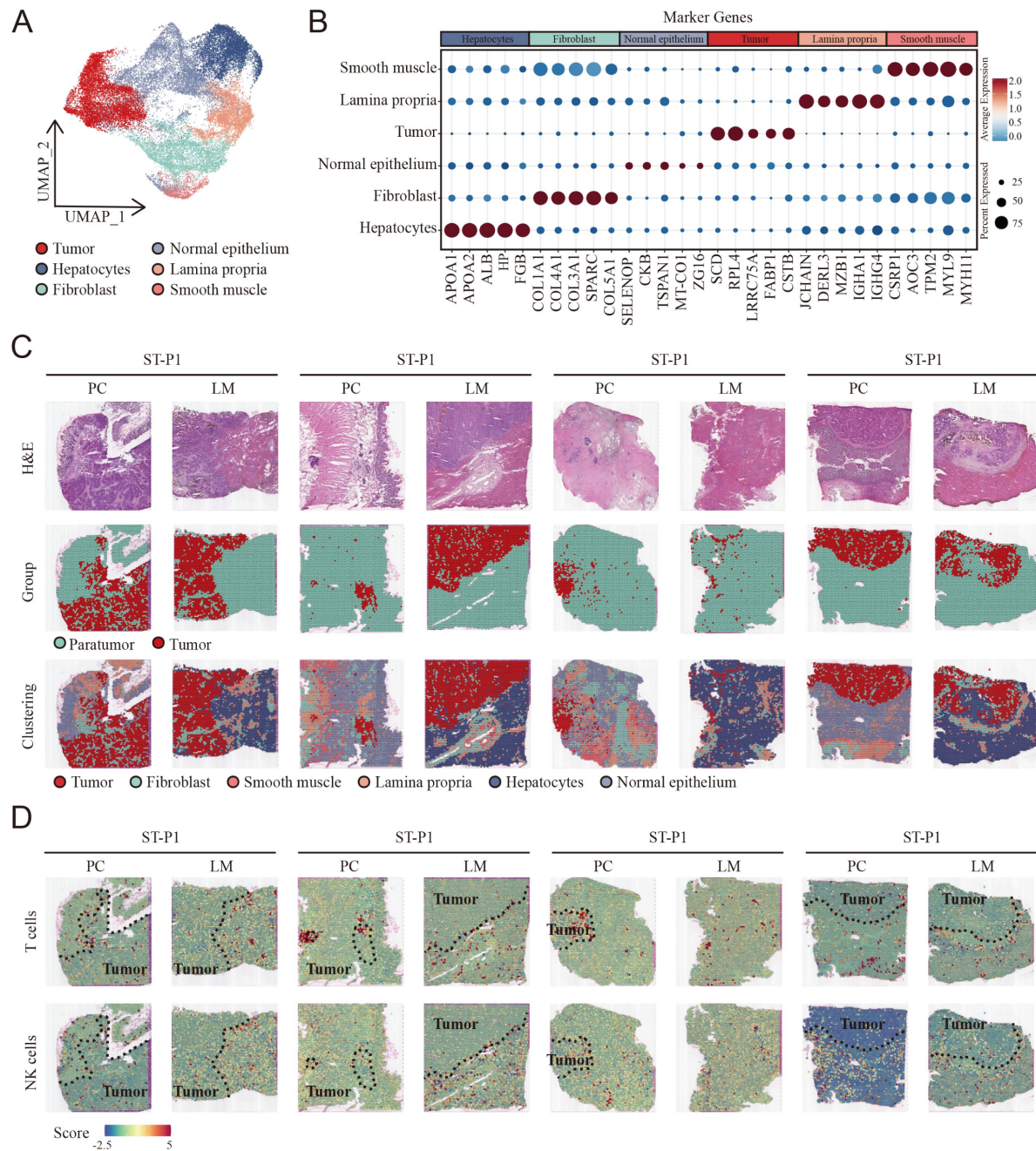


Figure 2.

Cellular identification in spatial transcriptomic samples. A. UMAP visualization of cell clusters in spatial transcriptomic samples. B. Dot plots showing average expression of markers in indicated cell clusters. C. Overview of the spatial transcriptomic sections. H&E staining of spatial transcriptomic sections (upper). Tumor tissue and paratumor tissue identification of each section (middle). Spatial cluster distribution of each section (lower). PC: primary cancer, LM: liver metastasis. D. The signature scores of T cells (upper) and NK cells (lower) in colon cancer and liver metastasis in the spatial transcriptomic sections.

To integrate the scRNA-seq and ST data, we used the AddModuleScore function in Seurat to quantify the main immune subpopulations. Consistent with scRNA-seq, T cells were remarkably enriched in the tumor region of both primary colon cancer and liver metastasis cancer, whereas NK cells were enriched in the non-tumor area (**Fig. 2D** [↗](#)).

Biological Relationship Between NK Cells and Metastasis of Colon Cancer Revealed by Bulk RNA Transcriptomics

TME cell composition differences between metastasis and non-metastasis colon cancer were evaluated using multiple tools that could robustly quantify the abundance of cell populations based on transcriptomic datasets, including xCell, EPIC, quanTIseq, and MCPcounter and bulk-seq datasets (TCGA COAD cohort). The percentages of NK cells markedly decreased in metastasis colon cancer using MCPcounter, EPIC, and xCell (**Fig. 3A-D** [↗](#)).

To further understand the potential triggers that induce colon cancer metastasis, the DEGs were calculated between the metastasis and non-metastasis colon cancer groups in the TCGA COAD cohort. A total of 1,378 DEGs were determined using the limma package with cutoffs $|\log \text{ fold change}| > 1.5$ and $p < 0.05$, including 817 upregulated and 561 downregulated genes between metastasis and non-metastasis colon cancer (**Fig. 3E** [↗](#)). Subsequently, GO and KEGG enrichment analyses and GSEA were performed to investigate the correlative functions and pathways. As shown in **Fig. 3F** [↗](#), cell killing, NK cell-mediated immunity, NK cell-mediated cytotoxicity, NK cell activation, and MHC-related GO terms were significantly enriched. The KEGG pathways of NK cell-mediated cytotoxicity were also enriched (**Fig. 3F** [↗](#)), with most of the genes in this pathway markedly downregulated in the metastasis group compared to the non-metastasis group. In contrast, GSEA revealed that NK cell-mediated cytotoxicity was enriched in the metastasis group (**Fig. 3G and H** [↗](#)).

The Landscape of NK Cells in CCLM Progression

The differences in infiltrated NK cells between tumor-adjacent tissues and tumor tissues suggest that the dynamic remodeling of NK cells may play an important role in CCLM progression. To further understand the landscape of NK cells in the CCLM microenvironments, NK cells were selected, and unsupervised clustering analysis was performed. Eight NK cell subtypes were thus identified (**Fig. 4A** [↗](#)). Combining the highly variable features of each NK cluster (**Fig. 4B** [↗](#)) and CIBERSORT-reported canonical NK cell markers (**Fig. 4C and D** [↗](#)), NK cells were classified into three cell types, including activated NK cells identified by the expression of KIR2DL4, GPR183, GRP171, CD69, and IFNG, resting NK cells marked by GZMK, TTC38, CD160, and PLEKHF1, and the other NK cells of which no characteristic gene was identified. Although all three NK cell subtypes were presented in primary colon tumors, adjacent normal colon tissues, liver metastasis tumors, and lymph nodes (**Fig. 4E** [↗](#)), the infiltration grade for each of these NK cell subsets was significantly different. At the individual sample level, considerable variability was observed in the NK cell subset composition. Where serial samples were available from individual patients, the expression of resting NK cells increased, whereas that of activated NK cells decreased during disease progression (**Fig. 4F and G** [↗](#)). Additionally, using the paired primary colon tumor, adjacent normal colon tissues, and liver metastasis tumor samples, we observed that the gradient of the resting NK cells increased, whereas the gradient of the activated NK cells decreased (**Fig. 4H** [↗](#)).

To evaluate the clinical relationship between NK cell differences and CCLM, CIBERSORT was performed using the TCGA COAD cohort. The percentages of resting NK cells significantly increased (**Fig. 5A** [↗](#)), and the activated NK cells decreased in the metastasis group (**Fig. 5B** [↗](#)), which is consistent with the scRNA-seq results. Also, we observed that the resting NK cells were significantly increased, whereas the activated NK cells decreased in higher T, N, and TNM stages (**Fig. S4A**). In terms of survival, neutrophils and resting NK cells were associated with a worse prognosis, whereas activated NK cells and M1 macrophages were associated with better outcomes

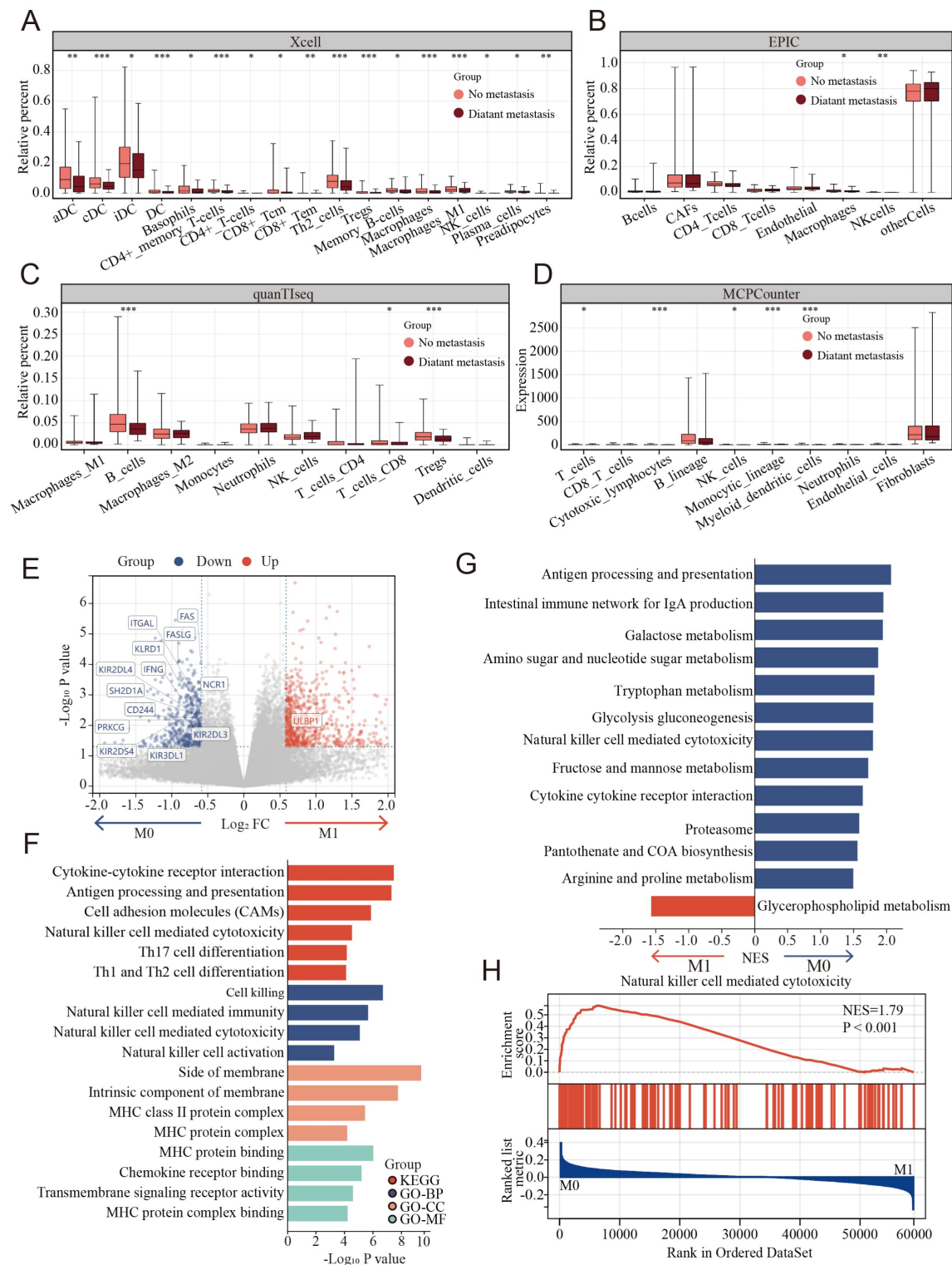


Figure 3.

Clinical and biological relationship between NK cells and metastasis of colon cancer revealed by Bulk RNA transcriptomics. A-D. The relationship of immune cell percentage determined by xCell, EPIC, quanTiseq and MCPCounter between metastasis and non-metastasis tumor in TCGA COAD cohort. E. Volcano plot showing differentially expressed genes between metastasis and non-metastasis colon cancer in TCGA COAD cohort. F. GO and KEGG enriched pathway bar chart of DEGs in metastasis versus non-metastasis colon cancer. G. Gene set enrichment analysis (GSEA) of KEGG gene set. H. Natural killer cell mediated cytotoxicity was enriched in the non-metastasis colon cancer.

(Fig. S4B). Further, survival analysis showed that colon cancer patients with lower and higher degrees of infiltration of activated NK cells and resting NK cells, respectively, had a significantly worse prognosis in the TCGA COAD and GSE29623 cohorts (**Fig. 5C and D**). Interestingly, resting NK cells were remarkably enriched in the tumor region, whereas activated NK cells were enriched in the non-tumor area of both primary colon cancer and liver metastasis (**Fig. 5E**).

Characterization and Developmental Course of Differential Subsets of NK Cells in CCLM

To further study the heterogeneity of NK cells subgroup, the proportions of all eight clusters of NK cells were calculated (Fig. S5). KIR2DL4⁺ GPR171⁺ activated NK cells were lessened in proportion with the progression of the disease from normal colon to colon cancer and liver metastasis cancer, whereas GZMK⁺ resting NK cells increased (**Fig. 6A and B**), suggesting that these two NK subsets were associated with metastasis. ST analysis also confirmed that there was more infiltration of the KIR2DL4⁺ GPR171⁺ activated NK cell subset in the non-tumor area and GZMK⁺ resting NK cells in the tumor region, both primary colon cancer and liver metastasis (**Fig. 6C**).

Pseudotime cell trajectory analysis of the two NK cell clusters was constructed to investigate the evolutionary dynamics of metastasis-associated NK cells. NK cells from the normal colon group were located at the top right corner of the trajectory curve, suggesting the clear starting point of this evolving trajectory curve. After confirmation of this starting point, developmental routes were determined to begin with the KIR2DL4⁺ GPR171⁺ activated NK cells and then develop into GZMK⁺ resting NK cells (**Fig. 6D**).

To explore the transitional relationships of marker genes in NK cells in distinct clusters, we examined the expression level of these markers in different clusters through pseudotime analysis. Marker genes of activated NK cells (KIR2DL4 and GPR171) exhibited a gradient descent expression pattern, whereas the expression of resting NK cell marker genes (GZMK) exhibited a gradient rise pattern (**Fig. 6E**). BEAM analysis was performed to identify the cell cluster marker genes that change as NK cell subtypes move from the activated stage to the resting stage. The branched heatmap showed the expression dynamics of the top 200 significant genes in different cell fate branches. Corresponding GO enrichment analyses of these significant genes further demonstrated that a mass of leukocyte differentiation and immune system process-related GO terms were significantly enriched (**Fig. 6F**).

Interestingly, patients with colon cancer with higher infiltration of GZMK⁺ resting NK cells (**Fig. 6G**) and lower infiltration of KIR2DL4⁺ GPR171⁺ activated NK cells (**Fig. 6H**) exhibited shorter survival in the TCGA COAD cohort.

Tumor Cells-Educated NK Cells Shift Toward Tumor-Promoting Status Depends on Cell-to-Cell Interaction

Given the characteristic spatial distribution of NK cell subpopulations, we hypothesized that the tumor region-enriched NK cells might be educated by tumor cells and thus functionally distinct. To verify the possible effect of tumor cells on the phenotypic switch of NK cells, we set up mixed cell co-culture experiments using colon cell line HCT-116 and NK cell line NK-92 in the ratio 1:1. As controls, NK cells were cultured alone, either in the tumor supernatant or fresh medium (Fig. S6A). After 24 h of co-culturing, NK cells were analyzed using FACS to determine the expression of the NK cells markers above identified as well as functional receptors NKG2A and NKG2D. Upon exposure to tumor cells, NK cells significantly decreased the expression of activated receptor KIR2DL4 (**Fig. 7A**) and functional receptors, both NKG2A and NKG2D (**Fig. 7B**). However, no such effect was observed after co-culturing with tumor supernatant and fresh medium.

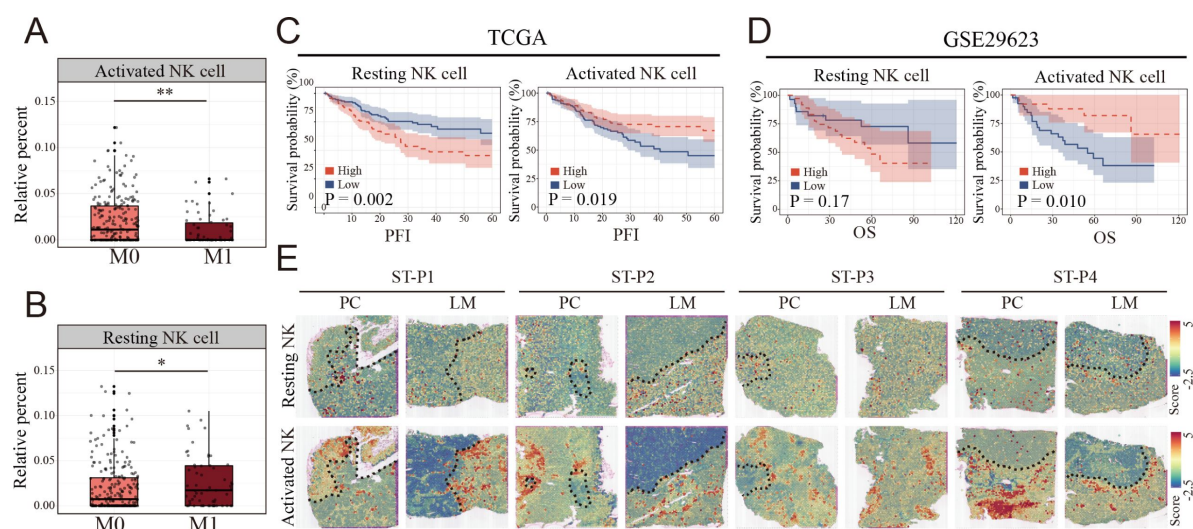


Figure. 5

Clinical relationship between NK cells subsets and metastasis of colon cancer revealed by Bulk RNA and spatial transcriptomics. A-B. The relationship of activated and resting NK cell percentage determined by CIBERSORT and tumor metastasis in TCGA COAD cohort. C-D. K-M survival plots show that high resting NK cell and low activated NK cell predicted poor prognosis in TCGA COAD and GSE29623 cohort. E. The signature scores of resting (upper) and activated NK cells (lower) in colon cancer and liver metastasis in the spatial transcriptomic sections.

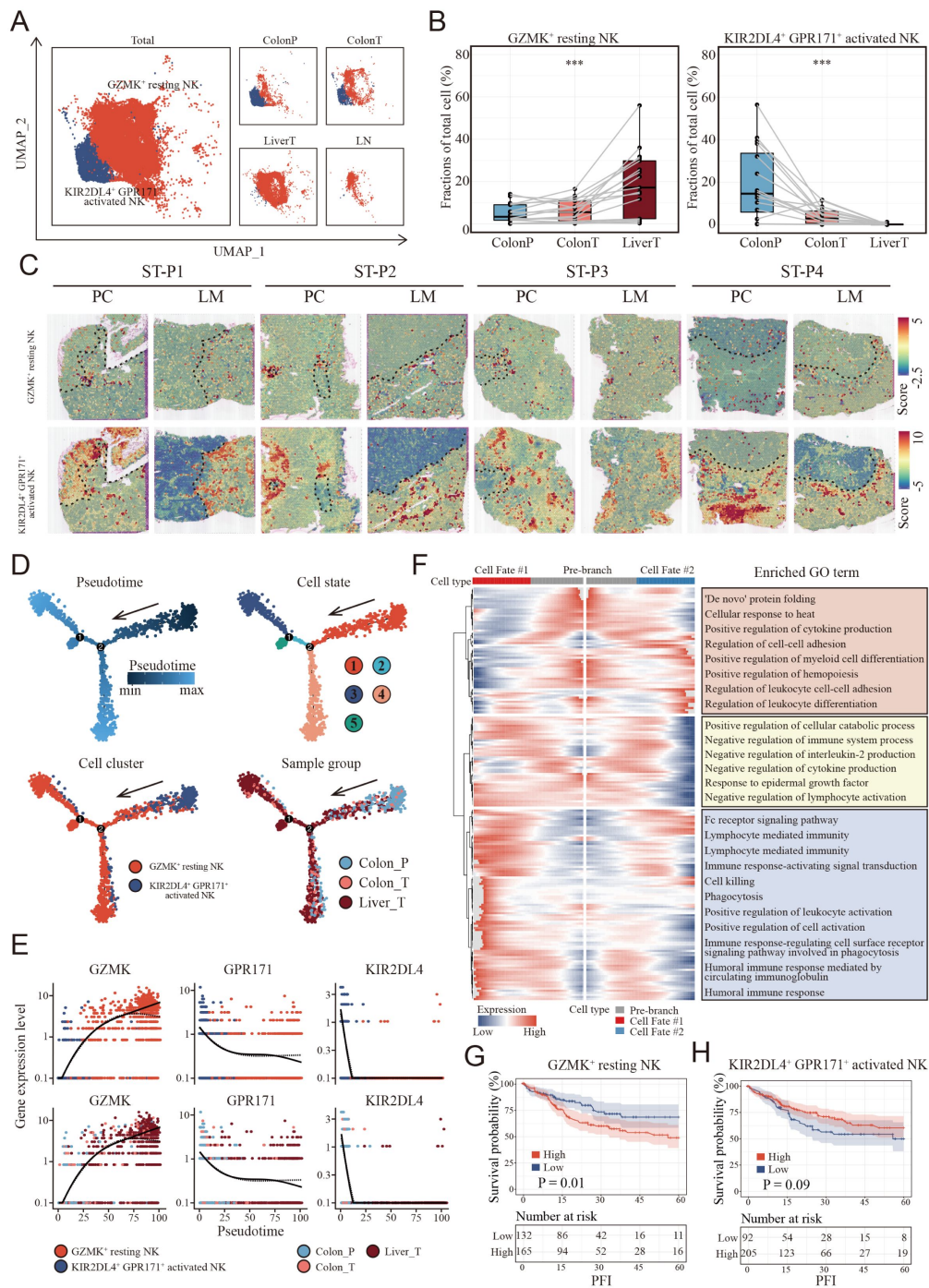


Figure 6.

Characterization and developmental course of differential subsets of NK cells in CCLM. **A**. The UMAP plot of KIR2DL4⁺ GPR171⁺ Activated NK cells, GZMK⁺ resting NK cells from CCLM. **B**. Proportions of KIR2DL4⁺ GPR171⁺ Activated NK cells, GZMK⁺ resting NK cells in total immune cells. P values were determined by the paired nonparameter test. **C**. The signature scores of GZMK⁺ resting NK cells (upper) and KIR2DL4⁺ GPR171⁺ Activated NK cells (lower) in colon cancer and liver metastasis in the spatial transcriptomic sections. **D**. Monocle analysis showing the developmental trajectory of NK cells. Color as in Pseudotime, cell state, subsets of NK cells and sample group. **E**. Pseudo-temporal change curve of marker genes in each subsets of NK cells. **F**. The heatmap shows the expression patterns of the top 50 significant genes in branched expression analysis modeling, associated GO terms (using DAVID v6.7) are given on the right of the corresponding gene clusters. **G-H**. The Kaplan-Meier curve shows COAD patients survival with different GZMK⁺ resting NK cells and KIR2DL4⁺ GPR171⁺ Activated NK cells infiltration.

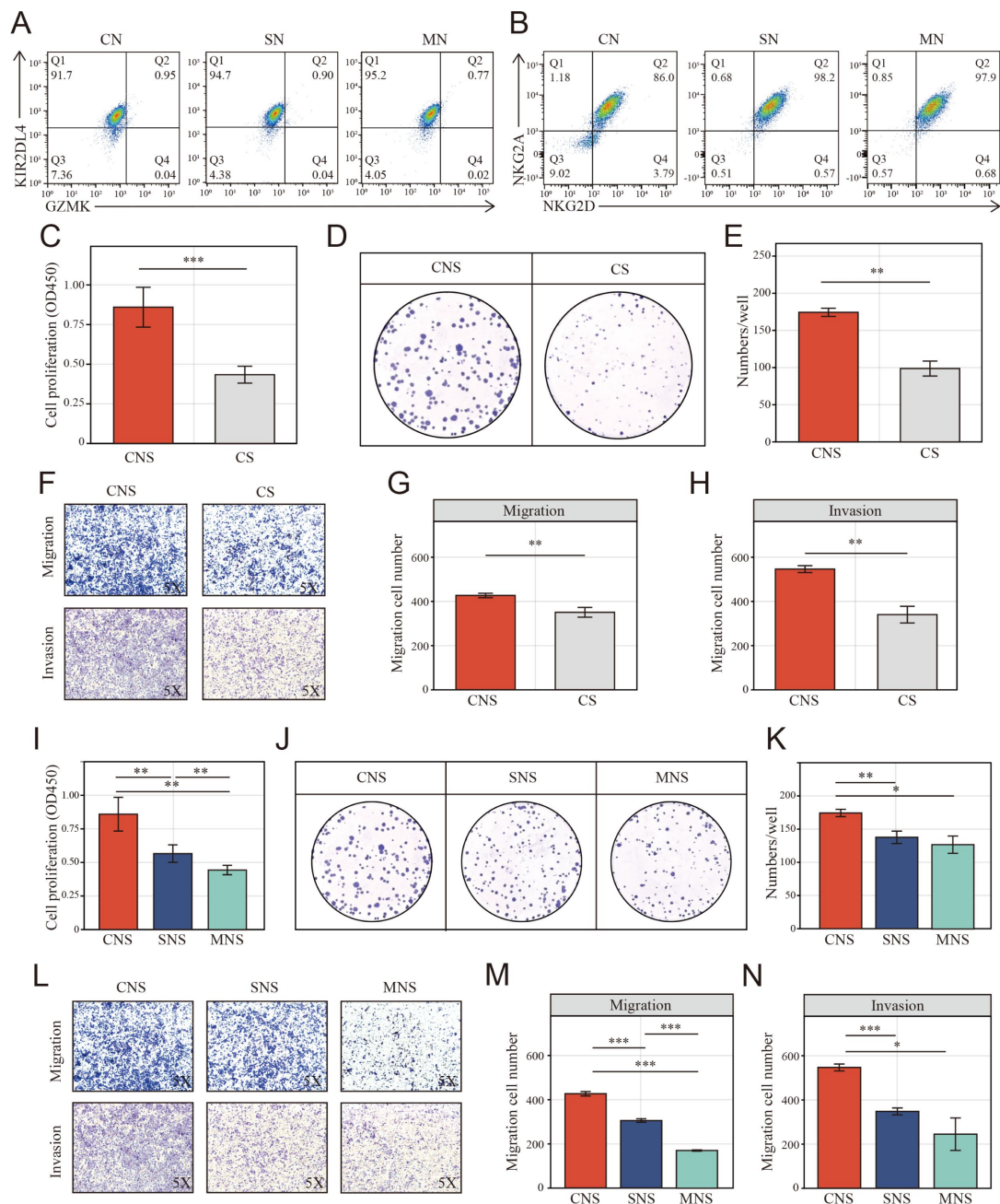


Figure. 7

Colon cancer cells (HCT-116) educated NK cells shift toward tumor promoting status depends on cell-to-cell interaction. A-B. Phenotype switch of NK cells were induced by cell-to-cell interactions with cancer cells. NK cells (NK-92) were cocultured with colon cancer cells (CN), supernatant of cancer cells (SN), or cultured alone (MN), and analyzed by FACS to evaluate the phenotype switch. C. CCK-8 assay showed the NK cell-mediated inductive effect on cell proliferation of colon cancer cell (HCT-116). Colon cancer cells were cultured in the supernatant from co-culture system that NK and cancer cells were cultured in the upper chamber (CNS); cancer cells cultured directly in supernatant that cancer cells were cultured in the upper chamber (CS). D-E. Clone formation assay showed the NK cell-mediated inductive effect on cell proliferation of colon cancer cell (HCT-116). F-H. The NK cell-mediated inductive effect on migration and invasion of colon cancer cell (HCT-116). I. CCK-8 assay showed the NK cell-mediated inductive effect on cell proliferation of colon cancer cell (HCT-116). Colon cancer cells were cultured in the supernatant from different co-culture system in transwell devices. NK cells were cultured with colon cancer cells in contact in the upper chamber of transwell (CNS), with supernatant of cancer cells (SNS), with fresh medium (MNS). J-K. Clone formation assay showed the NK cell-mediated inductive effect on cell proliferation of colon cancer cell (HCT-116). L-N. The NK cell-mediated inductive effect on migration and invasion of colon cancer cell (HCT-116).

To explore the NK cell-mediated inductive effect on colon cells, we performed co-culture experiments in transwells, and the co-cultured supernatant was collected to incubate fresh HCT-116 (Fig. S6B).

Interestingly, HCT-116 cells in the CNS group underwent a significant increase in proliferation (Fig. 7C-E) and migration (Fig. 7F-H) compared to the CS group, where cancer cells were cultured directly in the supernatant after 24 h of cancer cell culturing. Furthermore, CCK-8 (Fig. 7I) and colony formation assays (Fig. 7J-K) showed that colon cells underwent a significant increase in proliferation when cultured in the supernatant from the co-culture system in which NK and colon cells were in contact (CNS group), but not when co-cultures were performed in the cell supernatant (SNS group) and fresh medium (MNS group). Similarly, the migration and invasion of HCT-116 were significantly increased when cultured in the supernatant from the co-culture system in which NK and colon cells were in contact (CNS group) (Fig. 7L-N).

Further, another colon cancer cell line, DLD-1, was chosen to evaluate the effect of the supernatant in the different co-culture groups. DLD-1 cells in the CNS group did not undergo a prominent increase in proliferation, as HCT-116 and CCK-8 assays showed a minimal proliferation of colon cells in the MNS group (Fig. S7A-C). The same results were obtained for their migration and invasion (Fig. S7D-F). However, no such cell functional changes were induced in the CNS group (Fig. S7G-L).

Resting NK-induced Colon Cancer Malignant Phenotype Promotion Depends on SCF Release

To study the potential mechanism by which the supernatant from the NK and colon cells in direct contact with the co-culture system promoted colon cell migration, Luminex liquid suspension chip detection was used to compare the differential expression of 48 common chemotactic and inflammatory cytokines in the CNS, SNS, and MNS groups. We observed that SCF was upregulated in all three repetitions in the CNS group (Fig. 8A-B). Further, ELISA confirmed the upregulated level of SCF in the CNS group (Fig. 8C).

We further assessed the inhibitory effects of imatinib mesylate on the enhanced proliferation and invasion. CCK-8 (Fig. 8D-E) and colony formation assays (Fig. 8F-I) showed that imatinib mesylate (2 μ M) significantly inhibited supernatant-enhanced proliferation of HCT-116. Similarly, the supernatant-enhance migration (Fig. 8J-K) and invasion (Fig. 8L-M) were also inhibited by imatinib.

Discussion

CCLM is a multistep process and is mostly fatal (Manfredi et al., 2006). During disease progression, functional interactions between tumor cells and the surrounding TME are critical for influencing tumor growth, promoting angiogenesis, and finally resulting in metastasis (Quail et al., 2013). Since the genomic divergence between primary and metastatic CRC cells is relatively low (Wei et al., 2017; Yaeger et al., 2018) and accumulating evidence has highlighted the key role of tumor-infiltrating immune cells in dictating the fate of cancer cells (Kumar et al., 2018; Hanahan et al., 2012), we presented a comprehensive cellular and spatial immune landscape of the primary and liver metastatic tumors of CRC by using previously published scRNA-seq and ST data. Consistent with previous studies (Zhou et al., 2021; Wu et al., 2022), we observed that the immune microenvironment of primary and liver metastasis lesions of colon cancer had undergone extensive remodeling with a significantly decreased proportion of NK cells and a strong enrichment of T cells. However, the contrast between the decreased proportion of NK cells in tumor tissue and the enrichment of NK cells in tumor regions may indicate the specific effects of NK cells in CCLM.

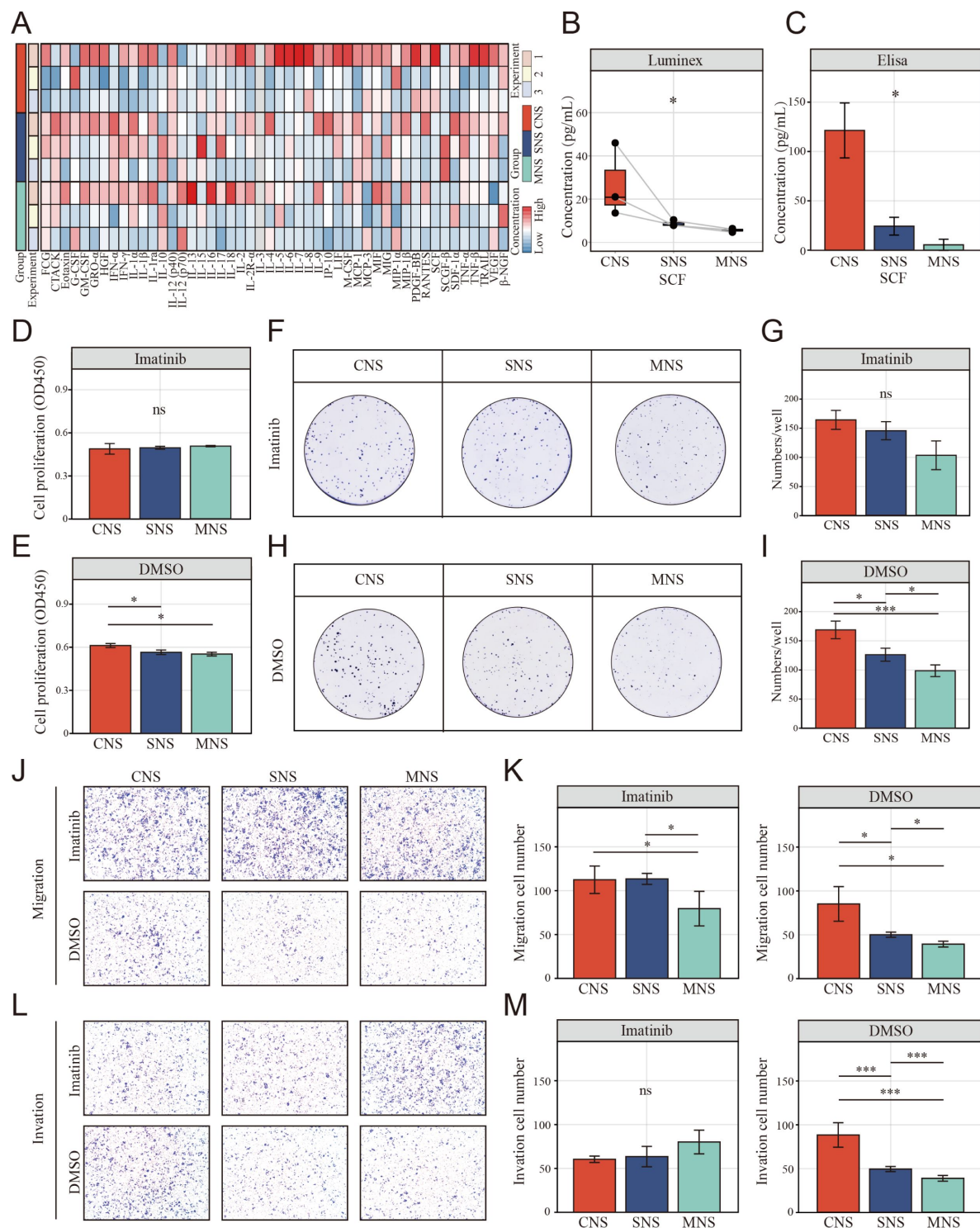


Figure. 8

The resting NK cell promote tumor malignant phenotype via elevating tumor-derived sSCF. A. luminex liquid suspension chip detection of 48 common chemotactic and inflammatory cytokines in CNS, SNS and MNS group. B-C. Concentration of SCF determined by luminex liquid suspension chip and Elisa in CNS, SNS and MNS group. D-E. CCK-8 assay showed the proliferation of HCT-116 cells was inhibited by imatinib mesylate, evaluated by a CCK-8 assay. Cells were incubated in the supernatant from different co-culture system with DMSO or 2 μ M imatinib mesylate. F-I. Clone formation assay showed the proliferation of HCT-116 cells was inhibited by imatinib mesylate. J-M. The NK cell-mediated inductive effect on migration and invasion of HCT-116 was inhibited by imatinib mesylate.

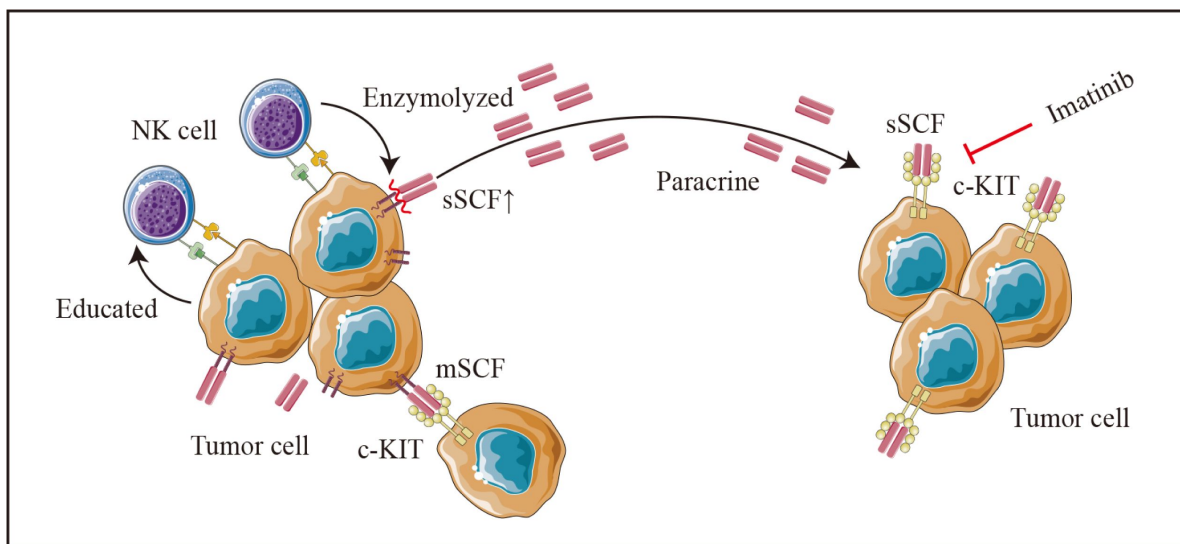


Figure. 9.

Schematic diagram. Colon cancer cells (HCT-116 cells) educate NK cells as resting status depends on cell-to-cell interaction. Tumor-educated NK cells subsequent enhances tumor malignancy in a paracrine manner by elevating tumor-derived sSCF.

Traditionally, NK cells within the TME were known as potential suppressors for tumor growth by directly killing cells and secreting proinflammatory cytokines (Huntington et al., 2007, Freud et al., 2006). However, the function of NK cells highly depends on their maturation status and localization (Cooper et al., 2001 [↗](#)). The peripheral blood CD56^{dim}CD16^{high} NK cell population predominantly mediates the killing of target cells by secreting perforin and granzymes (Jacobs et al., 2001 [↗](#)), whereas the CD56^{bright}CD16^{low} NK cells that reside in secondary lymphoid tissues are immature and have reduced cytotoxic capability (Moretta, 2010 [↗](#)). Recently, tumor-associated NK cells, which are enriched in tumors with impaired anti-tumor functions, were discovered to be associated with an unfavorable prognosis and resistance to immunotherapy in multiple solid tumors (Tang et al., 2023 [↗](#)), such as lung cancer, pancreatic cancer, and esophageal cancer. The potential impact of NK cells on CCLM progression is still poorly investigated.

In this study, the proportion of NK cells was higher than in past cognition, similar to a previous study (Xia et al., 2022 [↗](#)) in that NK cells occupied the largest immune cell compartment of nearly 50% in cholangiocarcinoma. In contrast, NK cells may not be well distinguished during automatic annotation using SingleR. Consistent with the study that revealed that treatment responders are associated with TME remodeling, including NK cell recruitment (Kim et al., 2022 [↗](#)), the proportions of NK cells in PR patients were significantly higher among the LiverP and LiverT groups (Fig. S1D and E), which also increased the overall proportion of NK cells to some extent. Additionally, we observed that NK cells are decreased in primary colon cancer and liver metastatic using scRNA-seq, consistent with previous findings supporting that NK cells play a crucial role in anticancer immunity (Laskowski et al., 2022 [↗](#), Myers et al., 2021). However, we further subdivided NK cells considering the conflicting result, in which NK cells were significantly enriched in the tumor area when using ST. Since this is the first study to comprehensively explore the heterogeneity of NK cells, no previous NK cell subpopulation markers were available; resting and activated NK cell markers in CIBERSORT were thus used to annotate NK cells. Consistent with a recent study that reported that mature and immature NK cells serve different functions (Thacker et al., 2023 [↗](#)), our results also provide evidence that resting NK cells in the colon cancer TME possess a potential tumor-promoting activity, whereas activated NK cells play an anti-tumor role as conventional cognition. Bulk RNA-sequencing and the corresponding clinical data further indicated that higher infiltration of resting NK cells and lower infiltration of activated NK cells were correlated with a worse prognosis in patients with CRC. However, since the resting and activated NK cells we identified were only the aggregation of multiple NK cell subpopulations, further studies are required to investigate the key NK cell subpopulations that play a crucial role in CCLM.

Further analysis of NK cell subtypes revealed a dramatic change in KIR2DL4⁺ GPR171⁺ activated NK cells and GZMK⁺ resting NK cells, whereas no other NK cell subpopulations differed in colon cancer progression. KIR2DL4, also known as CD158d, is an unusual member of the killer cell Ig-like receptor family expressed in all NK cells (Andre et al., 2001 [↗](#)). Studies revealed that KIR2DL4 activates the cytotoxicity of NK cells (Faure et al., 2002), and NK-92 cells stimulated with KIR2DL4 had higher cytotoxicity against breast cancer cells (Kilic et al., 2023 [↗](#)). Consistent with previous studies, we also observed that the expression of the KIR2DL4⁺ GPR171⁺ activated NK cell subtype was decreased during CCLM progression, possibly reflecting the anti-tumor activity of this population. However, the GZMK⁺ resting NK cell subsets were first identified as potential tumor promoters. Moreover, it has been proven that GZMK^{high} CD8⁺ T effector memory cells, a cell subset that is particularly similar to GZMK⁺ NK cells, were associated with poor clinical outcomes in patients with colorectal tumors. Our results also showed that GZMK⁺ resting NK cells highly infiltrate the cancer region, and this predicts a worse prognosis in patients with colon cancer. However, despite the interesting and gratifying clinical relevance, the mechanism remains unknown.

Considering the evolutionary trajectory and the characteristic distribution of these metastasis-associated NK cell subtypes, we predicted that activated NK cells might differentiate into resting NK cells under the action of tumor cells. Consistent with a recent study that indicated that exposure to cancer cells causes NK cells to lose their cytotoxic ability (Chan, Knutsdottir, 2020), we identified the tendency of NK cells to differentiate to an resting state with decreasing expression of activated marker KIR2DL4 as well as typical functional NK cell markers: NKG2D (Yu et al., 2023 [DOI](#)) and NKG2A which are only triggered by cell-to-cell interactions as validated by FACS. Unfortunately, resting markers GZMK can not be detected in all the three groups since it's a secreted protein.

Additionally, NK-mediated tumor cell editing appears to partly depend on the release of cytokines in in vitro co-culture experiments. SCF, the natural ligand of c-Kit with membrane-bound (mSCF) and soluble forms (sSCF) (Hsu et al., 1997 [DOI](#)), enhances the growth and migration of cancer cells such as cervical cancer (Aguilar et al., 2014 [DOI](#)), Ewing's sarcoma (Landuzzi et al., 2000 [DOI](#)) and CRC (Yasuda et al., 2007 [DOI](#)). Although the dimeric mSCF is remarkably more active and induces a more persistent activation of the receptor (Hsu, Wu, 1997, Langley et al., 1993 [DOI](#)), the tumor-promoting effect of the supernatant from the co-culture system in the current study and the reversion effect of imatinib for the co-culture supernatant induced pro-oncogenic effects suggests an important role of sSCF on colon cancer cells. However, no up-regulation of KITLG (the SCF encoding gene) was found in HCT-116 after co-culturing with NK cells (Fig. S9A). In addition, when using DLD-1, a colon cancer cell with a nearly 15 times lower expression of KITLG than HCT-116 (Fig. S9B), we also did not observe co-cultured supernatant induced tumor-promoting effects. We thus hypothesized that in our experimental system, NK cells may promote the cleavage and release of the extracellular part of SCF on the tumor cell surface after direct contact with tumor cells, and thus increase the concentration of sSCF, which induces the malignant phenotype of colon cancer cells in a paracrine manner (Fig. 8J [DOI](#)). However, the detailed mechanism still needs to be further studied.

In summary, we have unveiled the spatial and cellular profiles of TME from tumors and paratumor tissues of CCLM. Our analysis uncovered the different states, functions, and dynamic nature of NK cells in different CCLM settings, which can be used for further identification of regulatory mechanisms and for developing potential therapeutic targets.

Materials and Methods

Single-cell RNA Sequencing Analysis

The R (v4.0.5) package Seurat (v4.1.0) (Hao et al., 2021 [DOI](#)) was used to process the scRNA data. Since dataset quality control had been performed and Seurat objects had been created in previous studies, we did not further filter the scRNA-seq data or remove the batch effects. The SCTransform method was used to normalize the data. After selecting 2,000 highly variable genes using the FindVariableFeatures function in Seurat, principal component analysis was performed using these genes to reduce the data dimensions. Based on the ElbowPlot function in Seurat, we chose the top 30 principal components to run the FindNeighbors function. Next, the cells were clustered using the FindClusters function with a resolution of 0.1 for clustering immune cells. A uniform manifold approximation and projection algorithm was used for data visualization, as previously reported (Peng et al., 2023 [DOI](#)). Differentially expressed genes (DEGs) of each subset were identified using the FindAllMarkers function in Seurat. SingleR (v1.0.0) was used to name each cluster (Zheng et al., 2021 [DOI](#)).

Pseudotime Analysis

To analyze the differentiations of NK cells, *monocle2* (<http://cole-trapnell-lab.github.io/monocle-release>), which uses an algorithm to learn the changes in gene expression sequences that each cell must undergo as part of a dynamic biological process (Hong et al., 2022), was used for pseudotime trajectory analysis to identify the transitional relationships among different clusters. The cells were reduced dimensionally using the DDRTree method, sequenced in pseudotime, and finally visualized (Qiu et al., 2017).

Bulk RNA-seq Data Analysis

The bulk transcriptome RNA-seq data and corresponding clinical data were obtained from The Cancer Genome Atlas of colon adenocarcinoma through the UCSC Xena browser (GDC hub) (<https://gdc.xenahubs.net>) (Goldman et al., 2020). In total, 459 colon cancer samples with survival information were downloaded, and 310 samples were finally enrolled (11 formalin-fixed samples were excluded, and an additional 134 and 4 samples were excluded due to deletion of metastasis information and sequencing matrix, respectively). Transcriptomic data from 65 colon cancer samples in GSE29623 were obtained as the validation cohorts. CIBERSORT (Chen et al., 2018), xCELL (Aran et al., 2017), EPIC (Racle et al., 2017), and MCP-counter (Becht et al., 2016), which use gene expression to infer the proportions of tumor-infiltrating immune cells, were used to analyze the TME cell type. R packages *survival* (v3.2-10) and *survminer* (v0.4.9) were used for survival analysis. The Youden index was selected as the cutoff value to differentiate patients into distinct groups (high or low). The Kaplan–Meier survival curve was modeled using the *survfit* function. Subsequently, a Cox proportional hazards regression model was established to determine the independent risk factors. DEGs between the metastasis and non-metastasis groups were determined with the filtering condition of $\log_2 |\text{fold change}| > 1$ and $p\text{-value} < 0.05$, using the R package *limma*. GO and KEGG pathway functional enrichment analyses were performed using the *clusterProfiler* R package (v3.18.1) to assign various biological processes, molecular functions, cellular components, and pathways of identified marker genes in the cluster of interest (Yu et al., 2012), and $p < 0.05$ was regarded as statistically enriched. To explore the different KEGG pathways and hallmark gene sets between the metastasis and non-metastasis groups, gene set enrichment analysis (GSEA) was performed using data from The Molecular Signatures Database (c2.cp.kegg.v7.3.symbols) and the *fgsea* R package (v1.12.0) (Liberzon et al., 2015). Pathways with an adjusted $p\text{-value}$ below 0.05 were deemed to be significantly enriched.

ST Data Analysis

Seurat was also used for ST data processing and visualization. We used the SCT method to normalize the ST data; the functions *SelectIntegrationFeatures*, *PrepSCTIntegration*, *FindIntegrationAnchors*, and *IntegrateData* were used to integrate the ST data. An unsupervised clustering method was subsequently used to cluster similar ST spots. Cell population annotations were based on hematoxylin and eosin (H&E) staining sections and the highly variable genes in each cluster. Scores of cell-specific signatures (top 20 DEGs) from scRNA-seq were calculated using the *AddModuleScore* function. *SpatialDimPlot* and *SpatialFeaturePlot* were combined to visualize the cell expression level in the ST data (Peng, Ren, 2023).

Cell Lines and Co-cultures

Colon carcinoma cell lines HCT-116 and DLD-1 were purchased from the Cell Bank of the Chinese Academy of Sciences (Shanghai, China) and grown in a RPMI-1640 medium (GIBCO/BRL) supplemented with 10% FBS (GIBCO/BRL) in a humidified chamber at 37 °C and 5% CO₂. The human NK cell line NK-92 was also purchased from the Cell Bank of the Chinese Academy of Sciences (Shanghai, China) and maintained in RPMI-1640 supplemented with 12.5% horse serum (GIBCO), 12.5% FBS, 100 U/mL rhIL-2, 0.1 mmol/L β -mercaptoethanol, and 0.02 mmol/L folic acid.

Colon cancer cells were plated at a density of 1×10^5 cells/well in 6-well plates for 24 h. Supernatants were collected, and cells and debris were removed by centrifugation. NK cells were co-cultured with cancer cells in a ratio of 1:1 in a fresh mixed medium for a further 24 h. Additionally, NK cells were cultured in the soluble supernatant for 24 h with a supernatant/RPMI-1640 10% FBS and NK medium in the ratio 1:1. When indicated, co-cultures were performed in Transwell devices (JET biofil), maintaining the same ratios and culture times.

Flow Cytometry Analysis

NK cells in each co-cultured group were collected and washed twice in $1 \times$ PBA. Then, they were incubated with PE-labeled KIR2DL4 (Affinity Biosciences), FITC-labeled GZMK (Affinity Biosciences), FITC-labeled NKG2A (Biolegend) and PE-labeled NKG2D antibody (Biolegend) for 30 min, rewashed, and resuspended in PBS. BD flow cytometry was used for detection.

Cell Counting Kit-8 (CCK-8) Cell Viability and Cell Colony Formation Assay

Colon cancer cells (5,000 cells/well) were cultured in 96-well plates with co-cultured supernatants from different co-culture groups alone or with both co-cultured supernatants and imatinib mesylate (2 μ M) as previously reported (Yasuda, Sawai, 2007) for 24 h. At pre-determined time points, 10 μ L of CCK-8 reagent (Dojindo, Japan) was added and incubated for 2 h at 37 °C, and then the absorbance was measured using a microplate reader (Thermo Scientific) at 450 nm. All experiments were carried out in triplicate.

For the cell colony formation assay, colon cancer cells (500 cells/well) were seeded in 12-well plates with co-cultured supernatants alone or with both co-cultured supernatants and imatinib mesylate at 37 °C for 1 week. Then, cell colonies were fixed with 4% paraformaldehyde for 10 min and stained with 0.5% crystal violet for 5 min. Cell colonies containing >20 cells were counted. All experiments were carried out in triplicate.

Transwell Migration/Invasion Assays

The polycarbonate membrane in the transwell chambers was coated with Matrigel (Corning, NY, USA). Next, we transferred 1×10^5 cells from the serum-free medium with or without imatinib mesylate into the top chamber, added co-cultured supernatants alone or with both co-cultured supernatants and imatinib mesylate in the bottom chamber, and incubated at 37 °C for 24 h. Then, we removed the non-invading cells on the top side of the membrane by scrubbing, fixed the migrating or invading cells at the bottom side of the membrane with 4% paraformaldehyde, and stained with 0.5% crystal violet. The number of cells was counted under a microscope (Leica, London, UK) from four randomly chosen fields per well to determine the number of cells in each group.

Total RNA Extraction and Quantitative Real-Time PCR (qPCR)

Total RNA was extracted from cells using TRIZOL reagent (Invitrogen, USA). RNA was reverse transcribed into cDNA using a PrimeScript RT Reagent Kit (Takara, Japan). qPCR was performed using QuantStudio™ Test Development Software (Thermo Scientific, Waltham, MA, USA) with SYBR Green qPCR Master Mix (EZBioscience, Roseville, MN, USA). The sequence of KITLG and housekeeping gene GAPDH primers is listed in Table S1. KITLG mRNA data were normalized to that of GAPDH.

Luminex Liquid Suspension Chip Detection and ELISA

Luminex liquid suspension chip detection was performed by Wayen Biotechnologies (Shanghai, China). The Bio-Plex Pro Human Chemokine Panel 48-plex kit was used in accordance with the manufacturer's instructions. Briefly, supernatants from different co-cultured groups were

incubated in 96-well plates embedded with microbeads for 1 h and then incubated with a detection antibody for 30 min. Subsequently, streptavidin-PE was added in each well for 10 min, and values were read using the BioPlex MAGPIX System (Bio-Rad). The Human SCF ELISA kit (Solarbio, China) was used according to the manufacturer's instructions.

Statistical Analysis and Visualization

All statistical analyses were performed using SPSS (v23.0; IBM SPSS, Chicago, IL, USA) and R (v4.0.5), and data visualization was performed on R packages Seurat (v4.1.0), ggplot2 (v3.3.5), ggsignif (v0.6.1), and pheatmap (v1.0.12).

Data Availability

The raw data of single-cell RNA sequencing and ST data (10X Genomics) were derived from previously published research at the website: <http://www.cancerdiversity.asia/scCCLM/> (Wu, Yang, 2022). And two bulk transcriptomics data of colon cancer were downloaded from TCGA cohort COAD at the website: <https://xena.ucsc.edu/> and NCBI's Gene Expression Omnibus with accession number GSE29623. All data generated or analyzed during this study are available from the corresponding author on reasonable request.

Funding

Funder	Grant reference number	Author
National Natural Science Foundation of China	32070151	Xian Shen
Key R&D Program of Zhejiang Province	2020C03029	Xiangyang Xue
Key R&D Program of Zhejiang Province	2021C03120	Xian Shen
the Zhejiang Provincial Natural Science Foundation Project	Q24H160147	Wangkai Xie
the Postdoctoral Fellowship Program of CPSF	GZC20231956	Wangkai Xie
the Wenzhou Municipal Science and Technology Bureau Program	Y2020215	Dan Xiang
The funders had no role in study design, data collection and interpretation, or the decision to submit the work for publication		

Acknowledgements

We thank Prof. Qiang Gao from Fudan University and Prof. Xiaoming Zhang from Shanghai Institute of Immunity and Infection, CAS for sharing the SC RNA sequencing and ST data. We thank Zhejiang Key Laboratory of New Techniques for Diagnosis and Treatment of Critical Diseases of Pancreas and Liver and Zhejiang International science and Technology Cooperation base for tumor transformation research for supporting this study. We thank Editage Group (<https://www.editage.cn/>) for polishing the draft of this manuscript.

Authors' Contributions

CCM and **YYC**: Conceptualization, experimental design and execution, data curation, method development, formal analysis, statistics, writing original draft, and editing the manuscript. **DX** and **TMZ**: conceptualization, data curation and method development. **DFM** and **ZH**: experimental design. **WKX** and **CL**: experimental design. **YXL** and **JYY**: Validation. **DX**, **MDL** and **XYX**: Experimental design, supervision, funding acquisition, and manuscript editing. **XS**: Conceptualization, supervision, writing manuscript, project administration.

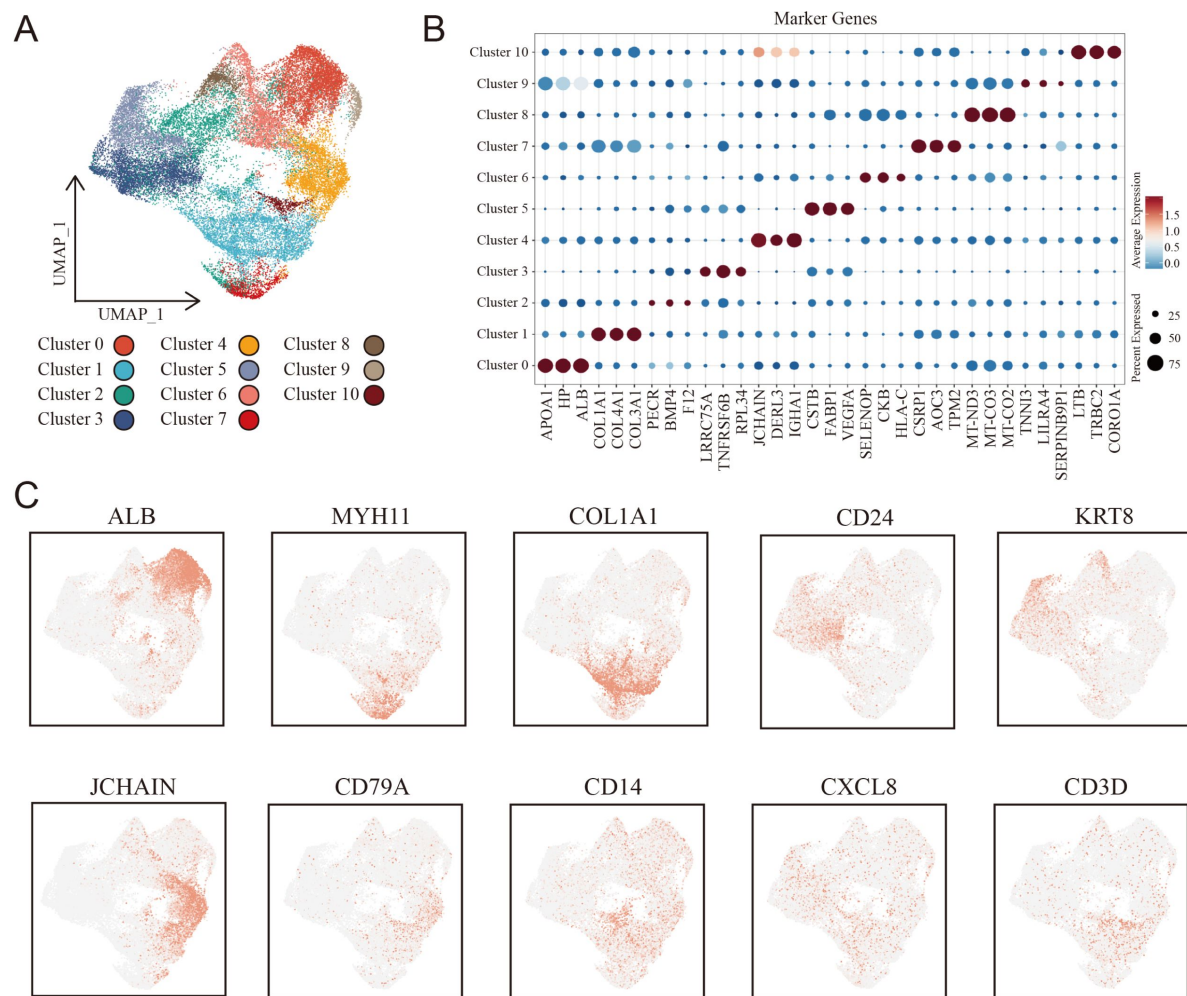


Figure S2.

Cellular identification in spatial transcriptomic samples.

A. The UMAP plot of all 11 cell clusters.

B. Dot plots showing average expression of marker genes in indicated cell clusters.

C. Expression of key markers across all samples.

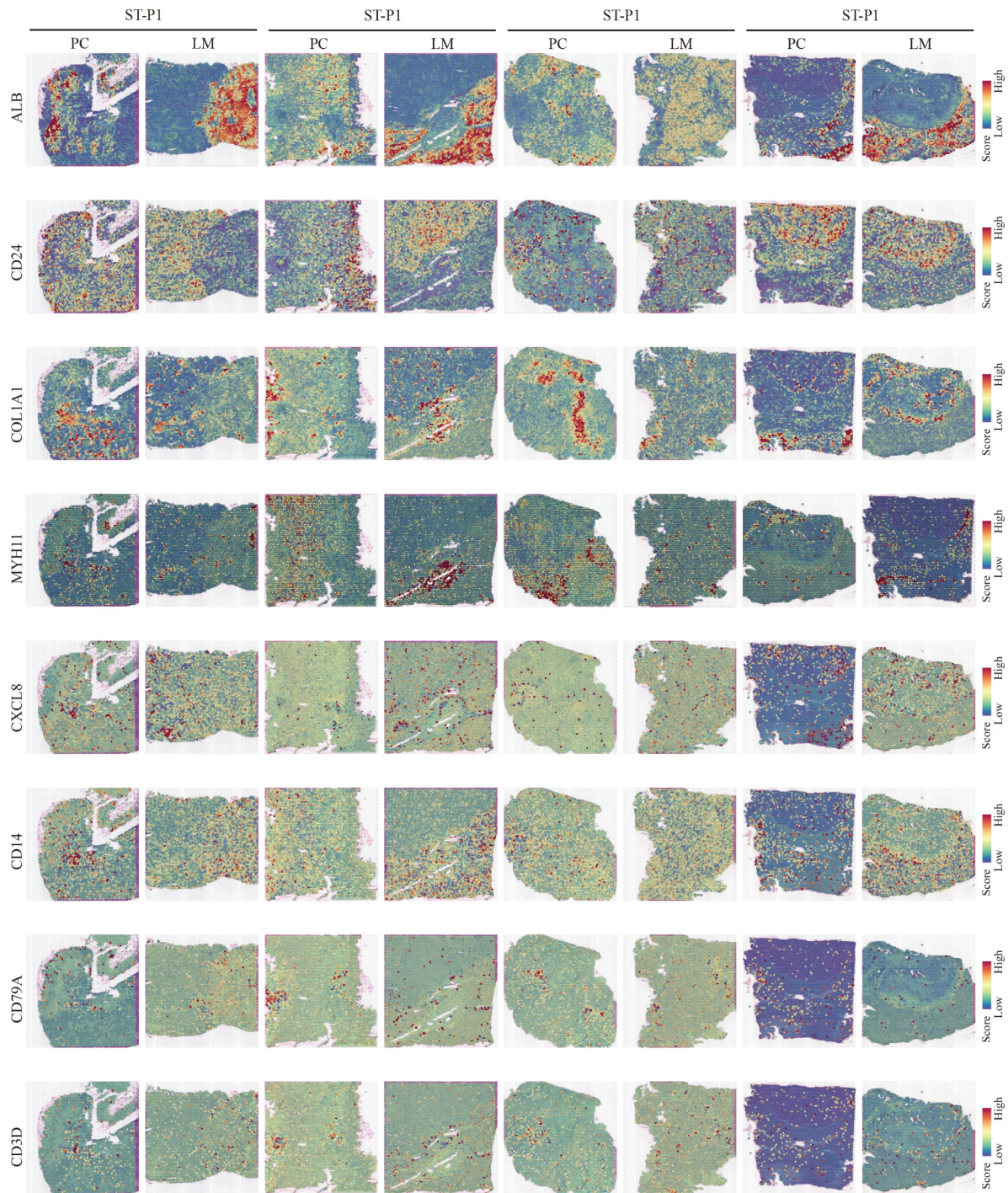


Figure S3.

Gene expression features of each sample.

The feature plots showed the expression distributions of ALB, CD24, COL1A1, MYH11, CXCL8, CD14, CD79A AND CD3D in each spatial transcriptomic section.

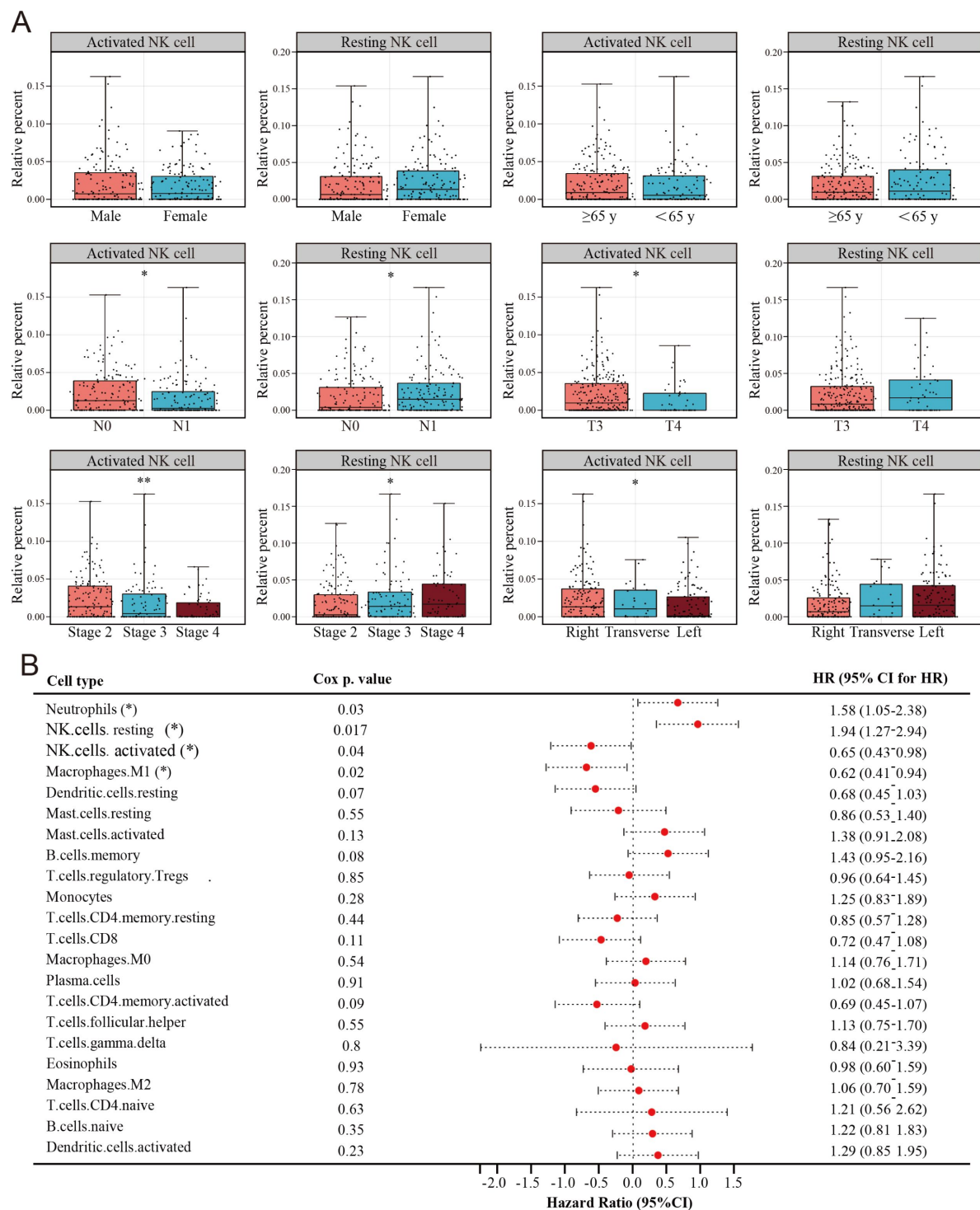


Figure. S4

Clinical relationship between NK cells subsets and colon cancer revealed by TCGA COAD cohort.

A. The relationship of activated and resting NK cell and clinical characteristics of colon cancer in TCGA COAD cohort.

B. The relationship of 22 immune cells percentage determined by CIBERSORT and prognosis of colon cancer in TCGA COAD cohort.

Figure. S5

The proportions of eight clusters of NK cells in Colon P, Colon T, Liver T and LN.

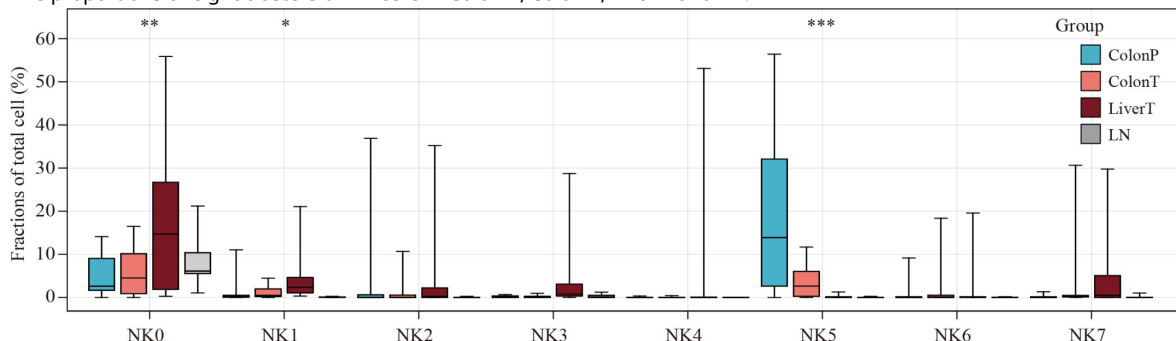
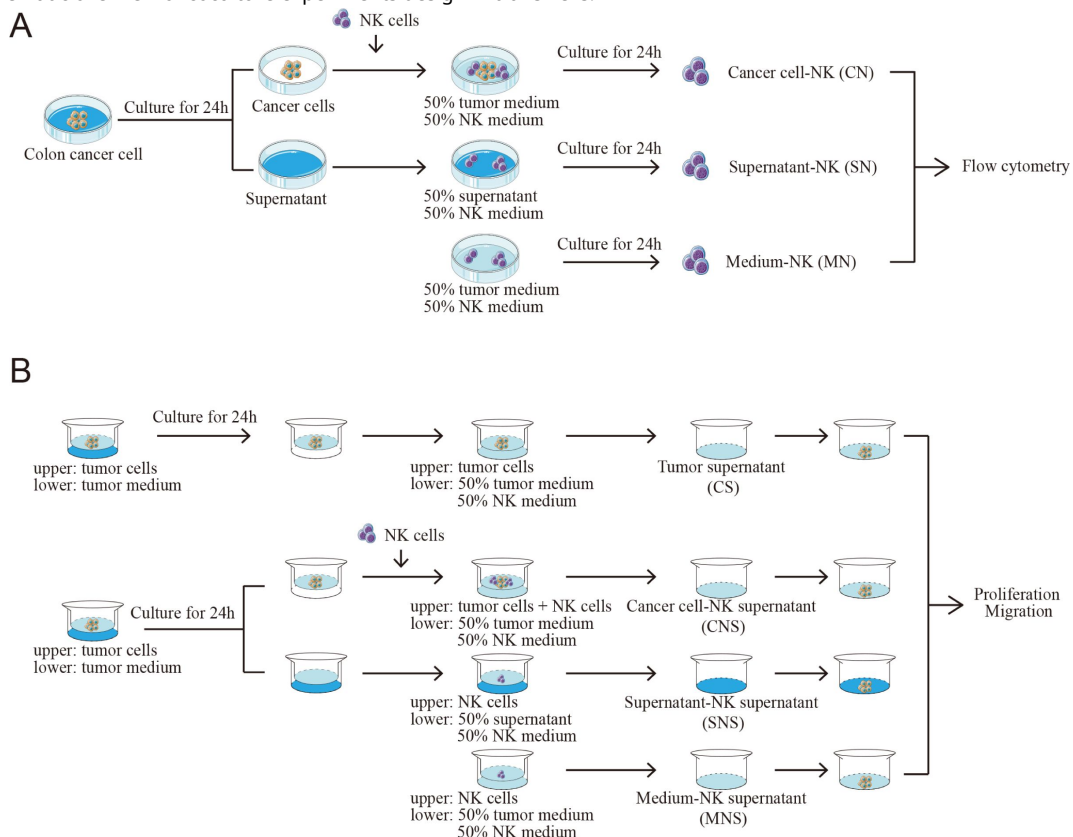


Figure. S6

Schematic overview of the in vitro experimental design.

A. Schematic overview of coculture experiments design.

A. Schematic overview of coculture experiments design in transwells.



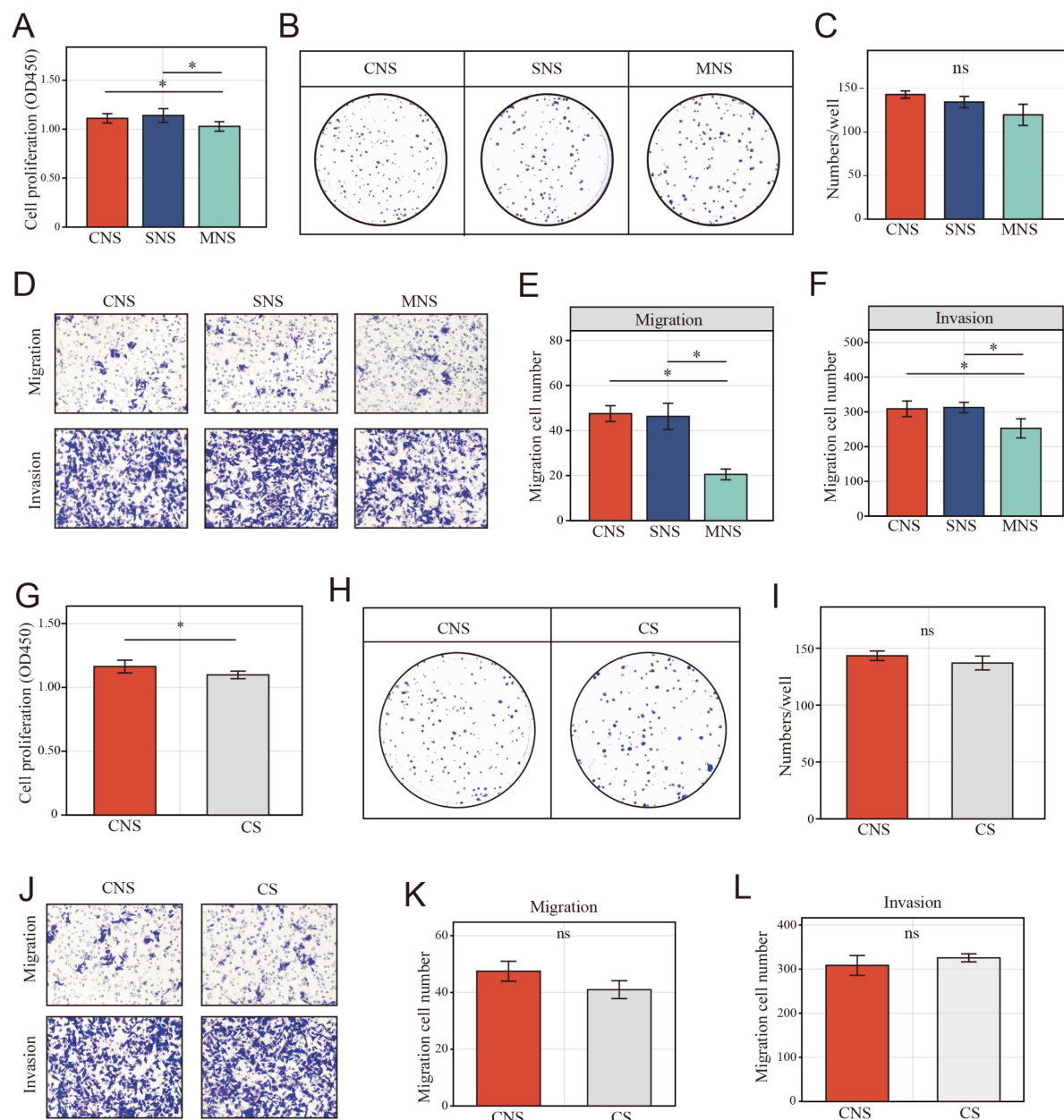


Figure. S7

NK cell-mediated tumor promoting effect in colon cancer cells (DLD-1).

A. CCK-8 assay showed the NK cell-mediated inductive effect on cell proliferation of DLD-1 cell among CNS, SNS, MNS groups.

B-C. Clone formation assay showed the NK cell-mediated inductive effect on cell proliferation of DLD-1 cell among CNS, SNS, MNS groups.

D-F. The NK cell-mediated inductive effect on migration and invasion of DLD-1 cell among CNS, SNS, MNS groups.

G. CCK-8 assay showed the NK cell-mediated inductive effect on cell proliferation of DLD-1 cell between CNS and CS groups.

H-I. Clone formation assay showed the NK cell-mediated inductive effect on cell proliferation of DLD-1 cell between CNS and CS groups.

J-L. The NK cell-mediated inductive effect on migration and invasion of DLD-1 cell between CNS and CS groups.

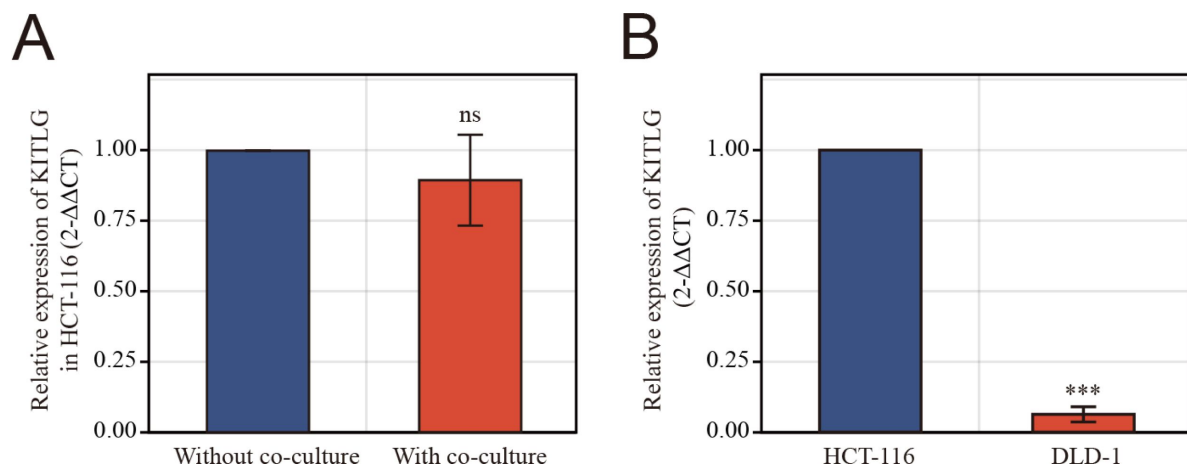


Figure. S8

Relative KITLG expression in different groups.

A. RT-qPCR analysis of KITLG expression in HCT-116 with and without co-cultured with NK cells.

B. RT-qPCR analysis of KITLG expression in HCT-116 and DLD-1 cells.

References

1. Sung H, Ferlay J, Siegel RL, Laversanne M, Soerjomataram I, Jemal A, Bray F (2021) **Global Cancer Statistics 2020: GLOBOCAN Estimates of Incidence and Mortality Worldwide for 36 Cancers in 185 Countries** *CA Cancer J Clin* **71**:209–49 <https://doi.org/10.3322/caac.21660>
2. Siegel RL, Miller KD, Goding Sauer A, Fedewa SA, Butterly LF, Anderson JC, Cercek A, Smith RA, Jemal A (2020) **Colorectal cancer statistics, 2020** *CA Cancer J Clin* **70** <https://doi.org/10.3322/caac.21601>
3. Wang F *et al.* (2023) **Single-cell and spatial transcriptome analysis reveals the cellular heterogeneity of liver metastatic colorectal cancer** *Sci Adv* **9** <https://doi.org/10.1126/sciadv.adf5464>
4. Chua TC, Saxena A, Chu F, Zhao J, Morris DL (2011) **Predictors of cure after hepatic resection of colorectal liver metastases: an analysis of actual 5- and 10-year survivors** *J Surg Oncol* **103**:796–800 <https://doi.org/10.1002/jso.21864>
5. Zampino MG *et al.* (2016) **Treatments for colorectal liver metastases: A new focus on a familiar concept** *Crit Rev Oncol Hematol* **108**:154–63 <https://doi.org/10.1016/j.critrevonc.2016.11.005>
6. Ruers T *et al.* (2017) **Local Treatment of Unresectable Colorectal Liver Metastases: Results of a Randomized Phase II Trial** *J Natl Cancer Inst* **109** <https://doi.org/10.1093/jnci/djx015>
7. Wancata LM, Banerjee M, Muenz DG, Haymart MR, Wong SL (2016) **Conditional survival in advanced colorectal cancer and surgery** *J Surg Res* **201**:196–201 <https://doi.org/10.1016/j.jss.2015.10.021>
8. Piawah S, Venook AP (2019) **Targeted therapy for colorectal cancer metastases: A review of current methods of molecularly targeted therapy and the use of tumor biomarkers in the treatment of metastatic colorectal cancer** *Cancer* **125**:4139–47 <https://doi.org/10.1002/cncr.32163>
9. Yao J, Chen Y, Lin Z (2023) **Exosomes: Mediators in microenvironment of colorectal cancer** *Int J Cancer* **153**:904–17 <https://doi.org/10.1002/ijc.34471>
10. Liu H, Wang Z, Zhou Y, Yang Y (2023) **MDSCs in breast cancer: an important enabler of tumor progression and an emerging therapeutic target** *Front Immunol* **14** <https://doi.org/10.3389/fimmu.2023.1199273>
11. Ngambenjawong C, Gustafson HH, Pun SH (2017) **Progress in tumor-associated macrophage (TAM)-targeted therapeutics** *Adv Drug Deliv Rev* **114**:206–21 <https://doi.org/10.1016/j.addr.2017.04.010>
12. Li S *et al.* (2019) **Tumor-associated neutrophils induce EMT by IL-17a to promote migration and invasion in gastric cancer cells** *J Exp Clin Cancer Res* **38** <https://doi.org/10.1186/s13046-018-1003-0>

13. Tiberti S *et al.* (2022) **GZMK(high) CD8(+) T effector memory cells are associated with CD15(high) neutrophil abundance in non-metastatic colorectal tumors and predict poor clinical outcome** *Nat Commun* **13** <https://doi.org/10.1038/s41467-022-34467-3>
14. Maskalenko NA, Zhigarev D, Campbell KS (2022) **Harnessing natural killer cells for cancer immunotherapy: dispatching the first responders** *Nat Rev Drug Discov* **21**:559–77 <https://doi.org/10.1038/s41573-022-00413-7>
15. Zhong F, Lin Y, Jing X, Ye Y, Wang S, Shen Z (2022) **Innate tumor killers in colorectal cancer** *Cancer Lett* **527**:115–26 <https://doi.org/10.1016/j.canlet.2021.12.022>
16. Villegas FR, Coca S, Villarrubia VG, Jimenez R, Chillon MJ, Jareno J, Zuñil M, Callol L (2002) **Prognostic significance of tumor infiltrating natural killer cells subset CD57 in patients with squamous cell lung cancer** *Lung Cancer* **35**:23–8 [https://doi.org/10.1016/s0169-5002\(01\)00292-6](https://doi.org/10.1016/s0169-5002(01)00292-6)
17. Ishigami S, Natsugoe S, Tokuda K, Nakajo A, Che X, Iwashige H, Aridome K, Hokita S, Aikou T (2000) **Prognostic value of intratumoral natural killer cells in gastric carcinoma** *Cancer* **88**:577–83
18. Lamb MG, Rangarajan HG, Tullius BP, Lee DA (2021) **Natural killer cell therapy for hematologic malignancies: successes, challenges, and the future** *Stem Cell Res Ther* **12** <https://doi.org/10.1186/s13287-021-02277-x>
19. Liu E *et al.* (2020) **Use of CAR-Transduced Natural Killer Cells in CD19-Positive Lymphoid Tumors** *N Engl J Med* **382**:545–53 <https://doi.org/10.1056/NEJMoa1910607>
20. Zhang H, Yang L, Wang T, Li Z (2024) **NK cell-based tumor immunotherapy** *Bioact Mater* **31**:63–86 <https://doi.org/10.1016/j.bioactmat.2023.08.001>
21. Hu W, Wang G, Huang D, Sui M, Xu Y (2019) **Cancer Immunotherapy Based on Natural Killer Cells: Current Progress and New Opportunities** *Front Immunol* **10** <https://doi.org/10.3389/fimmu.2019.01205>
22. Oh S, Lee JH, Kwack K, Choi SW (2019) **Natural Killer Cell Therapy: A New Treatment Paradigm for Solid Tumors** *Cancers (Basel)* **11** <https://doi.org/10.3390/cancers11101534>
23. Bruno A *et al.* (2013) **The proangiogenic phenotype of natural killer cells in patients with non-small cell lung cancer** *Neoplasia* **15**:133–42 <https://doi.org/10.1593/neo.121758>
24. Carrega P, Morandi B, Costa R, Frumento G, Forte G, Altavilla G, Ratto GB, Mingari MC, Moretta L, Ferlazzo G (2008) **Natural killer cells infiltrating human nonsmall-cell lung cancer are enriched in CD56 bright CD16(-) cells and display an impaired capability to kill tumor cells** *Cancer* **112**:863–75 <https://doi.org/10.1002/cncr.23239>
25. Zhang QF, Yin WW, Xia Y, Yi YY, He QF, Wang X, Ren H, Zhang DZ (2017) **Liver-infiltrating CD11b(-)CD27(-) NK subsets account for NK-cell dysfunction in patients with hepatocellular carcinoma and are associated with tumor progression** *Cell Mol Immunol* **14**:819–29 <https://doi.org/10.1038/cmi.2016.28>
26. Jin J, Fu B, Mei X, Yue T, Sun R, Tian Z, Wei H (2013) **CD11b(-)CD27(-) NK cells are associated with the progression of lung carcinoma** *PLoS One* **8** <https://doi.org/10.1371/journal.pone.0061024>

27. Chan IS *et al.* (2020) **Cancer cells educate natural killer cells to a metastasis-promoting cell state** *J Cell Biol* **219** <https://doi.org/10.1083/jcb.202001134>
28. Huergo-Zapico L *et al.* (2018) **NK-cell Editing Mediates Epithelial-to- Mesenchymal Transition via Phenotypic and Proteomic Changes in Melanoma Cell Lines** *Cancer Res* **78**:3913–25 <https://doi.org/10.1158/0008-5472.CAN-17-1891>
29. Manfredi S, Lepage C, Hatem C, Coatmeur O, Faivre J, Bouvier AM (2006) **Epidemiology and management of liver metastases from colorectal cancer** *Ann Surg* **244**:254–9 <https://doi.org/10.1097/01.sla.0000217629.94941.cf>
30. Quail DF, Joyce JA (2013) **Microenvironmental regulation of tumor progression and metastasis** *Nat Med* **19**:1423–37 <https://doi.org/10.1038/nm.3394>
31. Wei Q *et al.* (2017) **Multiregion whole-exome sequencing of matched primary and metastatic tumors revealed genomic heterogeneity and suggested polyclonal seeding in colorectal cancer metastasis** *Ann Oncol* **28**:2135–41 <https://doi.org/10.1093/annonc/mdx278>
32. Yaeger R *et al.* (2018) **Clinical Sequencing Defines the Genomic Landscape of Metastatic Colorectal Cancer** *Cancer Cell* **33**:125–36 <https://doi.org/10.1016/j.ccell.2017.12.004>
33. Kumar S, Wilkes DW, Samuel N, Blanco MA, Nayak A, Alicea-Torres K, Gluck C, Sinha S, Gabrilovich D, Chakrabarti R (2018) **DeltaNp63-driven recruitment of myeloid-derived suppressor cells promotes metastasis in triple-negative breast cancer** *J Clin Invest* **128**:5095–109 <https://doi.org/10.1172/JCI99673>
34. Hanahan D, Coussens LM (2012) **Accessories to the crime: functions of cells recruited to the tumor microenvironment** *Cancer Cell* **21**:309–22 <https://doi.org/10.1016/j.ccr.2012.02.022>
35. Zhou SN *et al.* (2021) **Comparison of Immune Microenvironment Between Colon and Liver Metastatic Tissue in Colon Cancer Patients with Liver Metastasis** *Dig Dis Sci* **66**:474–82 <https://doi.org/10.1007/s10620-020-06203-8>
36. Wu Y *et al.* (2022) **Spatiotemporal Immune Landscape of Colorectal Cancer Liver Metastasis at Single-Cell Level** *Cancer Discov* **12**:134–53 <https://doi.org/10.1158/2159-8290.CD-21-0316>
37. (2007) **Developmental pathways that generate natural-killer-cell diversity in mice and humans** *Nat Rev Immunol* **7**:703–14 <https://doi.org/10.1038/nri2154>
38. Freud AG, Caligiuri MA (2006) **Human natural killer cell development** *Immunol Rev* **214**:56–72 <https://doi.org/10.1111/j.1600-065X.2006.00451.x>
39. Cooper MA, Fehniger TA, Caligiuri MA (2001) **The biology of human natural killer-cell subsets** *Trends Immunol* **22**:633–40 [https://doi.org/10.1016/s1471-4906\(01\)02060-9](https://doi.org/10.1016/s1471-4906(01)02060-9)
40. Jacobs R, Hintzen G, Kemper A, Beul K, Kempf S, Behrens G, Sykora KW, Schmidt RE (2001) **CD56bright cells differ in their KIR repertoire and cytotoxic features from CD56dim NK cells** *Eur J Immunol* **31**:3121–7
41. Moretta L (2010) **Dissecting CD56dim human NK cells** *Blood* **116**:3689–91 <https://doi.org/10.1182/blood-2010-09-303057>

42. Tang F *et al.* (2023) **A pan-cancer single-cell panorama of human natural killer cells** *Cell* <https://doi.org/10.1016/j.cell.2023.07.034>
43. Xia T *et al.* (2022) **Immune cell atlas of cholangiocarcinomas reveals distinct tumor microenvironments and associated prognoses** *J Hematol Oncol* **15** <https://doi.org/10.1186/s13045-022-01253-z>
44. Kim R *et al.* (2022) **Early Tumor-Immune Microenvironmental Remodeling and Response to First-Line Fluoropyrimidine and Platinum Chemotherapy in Advanced Gastric Cancer** *Cancer Discov* **12**:984–1001 <https://doi.org/10.1158/2159-8290.CD-21-0888>
45. Laskowski TJ, Biederstadt A, Rezvani K (2022) **Natural killer cells in antitumour adoptive cell immunotherapy** *Nat Rev Cancer* **22**:557–75 <https://doi.org/10.1038/s41568-022-00491-0>
46. Myers JA, Miller JS (2021) **Exploring the NK cell platform for cancer immunotherapy** *Nat Rev Clin Oncol* **18**:85–100 <https://doi.org/10.1038/s41571-020-0426-7>
47. Thacker G *et al.* (2023) **Immature natural killer cells promote progression of triple-negative breast cancer** *Sci Transl Med* **15** <https://doi.org/10.1126/scitranslmed.abl4414>
48. Andre P *et al.* (2001) **New nomenclature for MHC receptors** *Nat Immunol* **2** <https://doi.org/10.1038/90589>
49. Faure M, Long EO (2002) **KIR2DL4 (CD158d), an NK cell-activating receptor with inhibitory potential** *J Immunol* **168**:6208–14 <https://doi.org/10.4049/jimmunol.168.12.6208>
50. Kilic N, Dastouri M, Kandemir I, Yilmaz E (2023) **The effects of KIR2DL4 stimulated NK-92 cells on the apoptotic pathways of HER2 + /HER-breast cancer cells** *Med Oncol* **40** <https://doi.org/10.1007/s12032-023-02009-6>
51. Yu L, Sun L, Liu X, Wang X, Yan H, Pu Q, Xie Y, Jiang Y, Du J, Yang Z. (2023) **The imbalance between NKG2A and NKG2D expression is involved in NK cell immunosuppression and tumor progression of patients with hepatitis B virus-related hepatocellular carcinoma** *Hepatol Res* **53**:417–31 <https://doi.org/10.1111/hepr.13877>
52. Hsu YR *et al.* (1997) **The majority of stem cell factor exists as monomer under physiological conditions. Implications for dimerization mediating biological activity** *J Biol Chem* **272**:6406–15 <https://doi.org/10.1074/jbc.272.10.6406>
53. Aguilar C, Aguilar C, Lopez-Marure R, Jimenez-Sanchez A, Rocha-Zavaleta L (2014) **Co-stimulation with stem cell factor and erythropoietin enhances migration of c-Kit expressing cervical cancer cells through the sustained activation of ERK1/2** *Mol Med Rep* **9**:1895–902 <https://doi.org/10.3892/mmr.2014.2044>
54. Landuzzi L *et al.* (2000) **The metastatic ability of Ewing's sarcoma cells is modulated by stem cell factor and by its receptor c-kit** *Am J Pathol* **157**:2123–31 [https://doi.org/10.1016/S0002-9440\(10\)64850-X](https://doi.org/10.1016/S0002-9440(10)64850-X)
55. Yasuda A, Sawai H, Takahashi H, Ochi N, Matsuo Y, Funahashi H, Sato M, Okada Y, Takeyama H, Manabe T (2007) **Stem cell factor/c-kit receptor signaling enhances the proliferation and invasion of colorectal cancer cells through the PI3K/Akt pathway** *Dig Dis Sci* **52**:2292–300 <https://doi.org/10.1007/s10620-007-9759-7>

56. Langley KE, Bennett LG, Wypych J, Yancik SA, Liu XD, Westcott KR, Chang DG, Smith KA, Zsebo KM (1993) **Soluble stem cell factor in human serum** *Blood* **81**:656–60
57. Hao Y *et al.* (2021) **Integrated analysis of multimodal single-cell data** *Cell* **184** <https://doi.org/10.1016/j.cell.2021.04.048>
58. Peng Z, Ren Z, Tong Z, Zhu Y, Zhu Y, Hu K (2023) **Interactions between MFAP5 + fibroblasts and tumor-infiltrating myeloid cells shape the malignant microenvironment of colorectal cancer** *J Transl Med* **21** <https://doi.org/10.1186/s12967-023-04281-6>
59. Zheng H, Liu H, Ge Y, Wang X (2021) **Integrated single-cell and bulk RNA sequencing analysis identifies a cancer associated fibroblast-related signature for predicting prognosis and therapeutic responses in colorectal cancer** *Cancer Cell Int* **21** <https://doi.org/10.1186/s12935-021-02252-9>
60. Hong B, Li Y, Yang R, Dai S, Zhan Y, Zhang WB, Dong R (2022) **Single-cell transcriptional profiling reveals heterogeneity and developmental trajectories of Ewing sarcoma** *J Cancer Res Clin Oncol* **148**:3267–80 <https://doi.org/10.1007/s00432-022-04073-3>
61. Qiu X, Hill A, Packer J, Lin D, Ma YA, Trapnell C (2017) **Single-cell mRNA quantification and differential analysis with CensuS** *Nat Methods* **14**:309–15 <https://doi.org/10.1038/nmeth.4150>
62. Goldman MJ *et al.* (2020) **Visualizing and interpreting cancer genomics data via the Xena platform** *Nat Biotechnol* **38**:675–8 <https://doi.org/10.1038/s41587-020-0546-8>
63. Chen B, Khodadoust MS, Liu CL, Newman AM, Alizadeh AA (2018) **Profiling Tumor Infiltrating Immune Cells with CIBERSORT** *Methods Mol Biol* **1711**:243–59 https://doi.org/10.1007/978-1-4939-7493-1_12
64. Aran D, Hu Z, Butte AJ (2017) **xCell: digitally portraying the tissue cellular heterogeneity landscape** *Genome Biol* **18** <https://doi.org/10.1186/s13059-017-1349-1>
65. Racle J, de Jonge K, Baumgaertner P, Speiser DE, Gfeller D. (2017) **Simultaneous enumeration of cancer and immune cell types from bulk tumor gene expression data** *Elife* **6** <https://doi.org/10.7554/eLife.26476>
66. Becht E *et al.* (2016) **Erratum to: Estimating the population abundance of tissue-infiltrating immune and stromal cell populations using gene expression** *Genome Biol* **17** <https://doi.org/10.1186/s13059-016-1113-y>
67. Yu G, Wang LG, Han Y, He QY (2012) **clusterProfiler: an R package for comparing biological themes among gene clusters** *OMICS* **16**:284–7 <https://doi.org/10.1089/omi.2011.0118>
68. Liberzon A, Birger C, Thorvaldsdottir H, Ghandi M, Mesirov JP, Tamayo P (2015) **The Molecular Signatures Database (MSigDB) hallmark gene set collection** *Cell Syst* **1**:417–25 <https://doi.org/10.1016/j.cels.2015.12.004>

Editors

Reviewing Editor

Florent Ginhoux

Singapore Immunology Network, Singapore, Singapore

Senior Editor

Paivi Ojala

University of Helsinki, Helsinki, Finland

Reviewer #1 (Public Review):

Summary:

Mao and colleagues re-analysed published spatial, bulk and single-cell transcriptomic datasets from primary colorectal cancers and colorectal-cancer-derived liver metastases. The analyses of paired cancer and non-cancer tissue samples showed that T cells are enriched in tumour tissue, accompanied by a reduction in the fraction of NK cells in the cancer tissue transcriptional datasets. Furthermore, authors claim that tumour tissue has a higher fraction of GZMK⁺ (resting) NK cells and suggest a correlation between the presence of these cells and poorer prognosis for cancer patients. In contrast, the increased frequency of KIR2DL4⁺ (activated) NK cells correlates with improved survival of cancer patients.

Strengths:

The authors performed a comprehensive analysis of published datasets, integrating spatial and single-cell transcriptomic data, which allowed them to discover the enrichment of GZMK⁺ NK cells in cancer tissues.

Weaknesses:

Despite their thorough analysis, the authors did not provide sufficient experimental evidence to support their claim that GZMK⁺ NK cells contribute to a worse prognosis for cancer patients or promote cancer progression. The terms resting and activated NK cells are used without properly defining the characteristics of these populations other than the gene expression of a handful of genes. Furthermore, the criteria used to quantify the NK cell population in spatial data is not entirely clear. While one can visually observe an increased fraction of GZMK⁺ NK cells compared to KIR2DL4⁺ NK cells in cancer tissues, no quantification is shown. They did not present any preclinical (animal model) or clinical data suggesting a causal relationship between NK cells and tumour growth. Thus, while a correlation may exist between the presence of GZMK⁺ NK cells and poorer tumour prognosis, causation cannot be claimed based on the available evidence. Furthermore, the in vitro data provided is limited to a single NK cell line derived from a lymphoma patient, which does not fully represent the diversity and functionality of human NK cells. Moreover, the in vitro experiments suffer from a lack of required controls and inadequate methodology.

<https://doi.org/10.7554/eLife.97201.1.sa1>

Reviewer #2 (Public Review):

Summary:

This manuscript investigates the role of the abundant NK cells that are observed in colon cancer liver metastasis using sequencing and spatial approaches in an effort to clarify the pro and anti-tumorigenic properties of NK cells. This descriptive study characterises different categories of NK cells in tumour and tumour-adjacent tissues and some correlations. An attempt has been made using pseudotime trajectory analysis but no models around how these NK cells might be regulated are provided.

Strengths:

This study integrates multiomics data to attempt to resolve correlates of protection that might be useful in understanding NK cell diversity and activation.

Weaknesses:

While this work is interesting, the power of such studies is in taking the discovered information and applying this to other cohorts to determine the strength and predictive power of the genes identified. It is also clear that these 'snapshots' analysed poorly take account of the dynamic temporal changes that occur within a tumour. It would have been good to see a proposed model of NK cell regulation as it might occur in the tumour (accounting for turnover and recruitment) beyond the static data.

<https://doi.org/10.7554/eLife.97201.1.sa0>